



PRESIDENCY UNIVERSITY

Private University Estd. in Karnataka State by Act No. 41 of 2013

Itgalpura, Rajankunte, Yelahanka, Bengaluru – 560064



MelanoSpectraNet: A Deep Learning Framework for Multi-Stage Melanoma Detection Using Hyperspectral Imaging

A PROJECT REPORT

Submitted by

Akhil Sanjay- 20221CSD0067

Jilpha Susmith- 20221CSD0066

S Arshiya- 20221CSD0129

Under the guidance of,

Dr. MADHUSUDHAN M V

BACHELOR OF TECHNOLOGY

IN

**COMPUTER SCIENCE AND ENGINEERING
(Data Science)**

PRESIDENCY UNIVERSITY

BENGALURU

DECEMBER 2025



PRESIDENCY SCHOOL OF COMPUTER SCIENCE AND ENGINEERING

BONAFIDE CERTIFICATE

Certified that this report “MelanoSpectraNet: A Deep Learning Framework for Multi-Stage Melanoma Detection Using Hyperspectral Imaging” is a Bonafide work of “Akhil Sanjay (20221CSD0067), Jilpha Susmith (20221CSD0066), S Arshiya (20221CSD0129)”, who have successfully carried out the project work and submitted the report for partial fulfilment of the requirements for the award of the degree of BACHELOR OF TECHNOLOGY in COMPUTER SCIENCE AND ENGINEERING, DATA SCIENCE during 2025-26.

Dr. Madhusudhan M V

Project Guide

PSCS

Presidency University

Dr. H M Manjula

Program Project

Coordinator

PSCS

Presidency University

Dr. Sampath A K

Dr. Geetha A

School Project

Coordinators

PSCS

Presidency University

Dr. S Pravindh Raja

Head of the Department

PSCS

Presidency University

Dr. Shakkeera L

Associate Dean

PSCS

Presidency University

Dr. Duraipandian N

Dean

PSCS & PSIS

Presidency University

Examiners

Sl.no.	Name	Signature	Date
1			
2			

PRESIDENCY UNIVERSITY

PRESIDENCY SCHOOL OF COMPUTER SCIENCE AND

ENGINEERING

DECLARATION

We the students of final year B.Tech in COMPUTER SCIENCE ENGINEERING, DATA SCIENCE at Presidency University, Bengaluru, named Akhil Sanjay, Jilpha Susmith, S Arshiya, hereby declare that the project work titled “MelanoSpectraNet: A Deep Learning Framework for Multi-Stage Melanoma Detection Using Hyperspectral Imaging” has been independently carried out by us and submitted in partial fulfilment for the award of the degree of B.Tech in COMPUTER SCIENCE AND ENGINEERING, DATA SCIENCE during the academic year of 2025-26. Further, the matter embodied in the project has not been submitted previously by anybody for the award of any Degree or Diploma to any other institution.

Akhil Sanjay USN: 20221CSD0067

Jilpha Susmith USN: 20221CSD0066

S Arshiya USN: 20221CSD0129

PLACE: BENGALURU

DATE:

ACKNOWLEDGEMENT

For completing this project work, We/I have received the support and the guidance from many people whom I would like to mention with deep sense of gratitude and indebtedness. We extend our gratitude to our beloved **Chancellor, Pro-Vice Chancellor, and Registrar** for their support and encouragement in completion of the project.

I would like to sincerely thank my internal guide **Dr. Madhusudhan M V, Associate Professor**, Presidency School of Computer Science and Engineering, Presidency University, for his moral support, motivation, timely guidance and encouragement provided to us during the period of our project work.

I am also thankful to **Dr. S Pravindh Raja, Professor, Head of the Department, Presidency School of Computer Science and Engineering** Presidency University, for his mentorship and encouragement.

We express our cordial thanks to **Dr. Duraipandian N**, Dean PSCS & PSIS, **Dr. Shakkeera L**, Associate Dean, Presidency School of computer Science and Engineering and the Management of Presidency University for providing the required facilities and intellectually stimulating environment that aided in the completion of my project work.

We are grateful to **Dr. Sampath A K, and Dr. Geetha A, PSCS** Project Coordinators, **Dr. Sharmasti vali, Program Project Coordinator**, Presidency School of Computer Science and Engineering, or facilitating problem statements, coordinating reviews, monitoring progress, and providing their valuable support and guidance.

We are also grateful to Teaching and Non-Teaching staff of Presidency School of Computer Science and Engineering and also staff from other departments who have extended their valuable help and cooperation.

AKHIL SANJAY
JILPHA SUSMITH
S ARSHIYA

Abstract

Out of all the skin cancers, melanoma is usually the one that is most likely to lead to the death of a human being. The reason for this is the fact that melanoma is a type of cancer that can spread rapidly if it is not detected at its very beginning. To a very large extent, the methods that are used for the diagnosis at the moment are mainly dependent on the visual inspection or surgical biopsies that sometimes may not be able to detect the changes that are subtle in the skin tissue. With the need for a faster, safer and more reliable screening methods growing a lot, this study focuses at the potential of Hyperspectral Imaging (HSI) to be a non-invasive tool that gives access to biochemical and structural information beyond what standard colour images can reveal.

This work suggests a deep learning-based system to identify the stages of melanoma clinically from hyperspectral volumetric data. HSI's primary goal is to obtain several pictures of the same lesion at different wavelengths. These pictures have very detailed spectral information and it is this that leads to the detection of the very first molecular changes associated with disease progression. In order to find the right patterns, a 3D U-Net architecture has been designed and trained which not only locates the area in the image that is most relevant, e.g. lesion boundaries, but also follows the pigment concentration, oxygenation, and depth characteristics that change in the tissue not only spatially but also spectrally.

The authors' architectural framework takes them through a well-organized procedure from raw to processed data and then advanced classification of different disease stages with volumetric deep convolutional layers by spectral–spatial feature enhancement. Their model demonstrates strong capability in distinguishing neighbouring melanoma stages which are very close situations and can hardly be differentiated by traditional imaging methods. The experiments conducted show constant improvements of the metrics in terms of precision, recall, and F1-score thus verification of the implemented method.

In fact, this work delivers a strong argument that utilizing the spectral hyperspectral data gotten by a 3D deep neural network might be a way to help doctors identify the disease at its earliest stages, reduce the cross-dependence on invasive procedures, and provide more accurate leukoderma assessment results. In achieving this model, the current work opens the door for eventual steps like larger datasets and spectral attention modules, or concatenation with other modalities.

Table of Content

Sl. No.	Title	Page No.
	Declaration	III
	Acknowledgement	IV
	Abstract	V
	List of Figures	VIII
	List of Tables	IX
	Abbreviations	X
1.	Introduction 1.1 Background 1.2 Statistics of project 1.3 Prior existing technologies 1.4 Problem Statement 1.5 SDGs 1.6 Overview of project report	1-12
2.	Literature review 2.1 Review of existing models 2.2 Research Gaps 2.3 Objectives	13-21
3.	Methodology	22-34
4.	Project management 4.1 Project timeline 4.2 Risk analysis 4.3 Project budget	35-39
5.	Analysis and Design 5.1 Requirements 5.2 Functional Block Diagram 5.3 System Flow Chart 5.4 System Design and Model Architecture 5.5 Data Pipeline and Preprocessing Design 5.6 Standards	40-53

	5.7 Mapping with IoTWF reference model layers 5.8 Domain model specification 5.9 Communication model 5.10 IoT deployment level 5.11 Functional view	
6.	Hardware, Software and Simulation 6.1 Computational Environment 6.2 Software development tools 6.3 Software code and Implementation Details 6.4 Simulation and Experimentation	54-67
7.	Evaluation and Results 7.1 Test points 7.2 Test plan 7.3 Test results 7.4 Insights and Recommendations	61-67
8.	Social, Legal, Ethical, Sustainability and Safety Aspects 8.1 Social aspects 8.2 Legal aspects 8.3 Ethical aspects 8.4 Sustainability aspects 8.5 Safety aspects 8.6 Collaborative and Education aspects 8.7 Future Adaptability and Scalability	68-72
9.	Conclusion	73-77
	References	78
	Base Paper	81
	Appendix	83

List of Figures

Figure	Caption	Page no
Fig 1.5.1	Sustainable development goals	10
Fig 3.1.1	V-Model Methodology	25
Fig 3.2.1	MelanoSpectraNet System Architecture	27
Fig 3.4.1	Unit Testing Flow	32
Fig 4.1.1	Gantt Chart of Project Timeline	37
Fig 5.2.1	Functional Block Diagram of MelanoSpectraNet	43
Fig 5.3.1	System Flow Chart of MelanoSpectraNet	44
Fig 5.4.1	3D U-Net Architecture Diagram	45
Fig 5.8.1	Domain Model for MelanoSpectraNet	50
Fig 5.9.1	Request Response Dataflow for MelanoSpectraNet	51
Fig 5.10.1	ML Deployment Level Adapted for MelanoSpectraNet	52
Fig 5.11.1	Functional View of MelanoSpectraNet	53
Fig 6.1.1	Diagram of Computational Hardware Stack	55
Fig 6.2.1	Diagram of Software Stack	56
Fig 6.3.1	Sample Code Block (Preprocessing Functions)	57
Fig 6.3.2	3D U-Net Model Definition	58
Fig 6.3.3	Training and Evaluation Loop	59
Fig A.1	Sample hyperspectral cube	84
Fig A.2	Example spectral profile from a melanoma region	84
Fig B.1	Full 3D U-Net architecture diagram	86
Fig B.2	Encoder-decoder schematic showing skip connections	87
Fig C.1	SNV normalization effect (before/after spectra)	89
Fig C.2	PCA Scree Plot showing variance retention	90
Fig C.3	Patch extraction visualization	91
Fig D.1	Accuracy curves	92
Fig D.2	Loss curves	93
Fig D.3	Example prediction vs ground truth	94

List of Tables

Table	Caption	Page no
Table 2.2.1	Summary of Literature reviews	18
Table 4.1.1	Project Planning Timeline	36
Table 4.2.1	Project Implementation Timeline	36
Table 4.2.1	PESTLE Analysis for the Project	38
Table 5.1.1	Summary of System Requirements	42
Table 5.7.1	Mapping MelanoSpectraNet with the IoTWF Reference Model	48
Table 5.8.1	Domain Model Description for MelanoSpectraNet	49
Table 7.1.1	Test points and measurements	62
Table 7.2.1	Test plan	63
Table 7.3.1	Confusion matrix	65
Table 7.3.2	Per class performance metrics	66
Table A.1	Dataset Overview	83
Table B.1	Training Configuration	88
Table C.1	PCA	91
Table D.1	Classification Performance	92

Abbreviations

Abbreviation	Full Form
AI	Artificial Intelligence
ANN	Artificial Neural Network
CNN	Convolutional Neural Network
DPDPA	Digital Personal Data Protection Act
GDPR	General Data Protection Regulation
GPU	Graphics Processing Unit
HSI	Hyperspectral Imaging
IoT	Internet of Things
ISO	International Organization for Standardization
PESTEL	Political, Economic, Social, Technological, Environmental, Legal
ML	Machine Learning
NIST	National Institute of Standards and Technology
PCA	Principal Component Analysis
RGB	Red, Green, Blue
SDG	Sustainable Development Goal
SNV	Standard Normal Variate
SVM	Support Vector Machine
TFL	TensorFlow (TF/Keras-based deep learning framework)
UN	United Nations
UNet	Convolutional Neural Network architecture with encoder-decoder structure
WHO	World Health Organization

Chapter 1

Introduction

Melanoma has been identified for years as one of the deadliest types of skin cancer, due to its rapid growth and potential to spread to distant sites throughout the body, rather than the frequency of occurrence. One of the first factors that contributes to the difficulty which is associated with diagnosing melanoma is its ability to replicate common moles or other innocuous pigmented macules in their early stages of cancer leading to underestimation by both patients and physicians alike [1]. As a result of the failure to diagnose melanoma early, the risk of the patient's mortality increases dramatically when the melanoma progresses beyond the confines of the epidermis.

The past twenty years has seen large advances in the use of technology to assist in the detection of melanoma in its initial stages, including the development of dermoscopy, digital imaging analysis software, and computer algorithms which utilize 2-dimensional images to identify suspicious skin lesions. Even though the advances described above have improved the likelihood of identifying melanoma, there continue to be limitations to early detection of this form of skin cancer. As of now, Dermatologists remain the primary diagnostician of melanoma, and the accuracy of diagnosis depends on the expertise and professional judgment of the physician. In many instances, ambiguity exists with regard to the diagnosis of melanoma; therefore, the burden of establishing a definitive diagnosis shifts to the performance of a biopsy procedure, which, although highly specific, is an invasive, time consuming, and often unnecessary process. Multiple studies have demonstrated that a high percentage of skin biopsies ultimately determine that the excised lesion was benign, resulting in unnecessary anxiety for the patient, unnecessary medical expense, and potentially unnecessary scarring [2].

Clinical challenges in diagnosing melanoma have made researchers focus their efforts on developing an imaging modality that detects skin cancer at an earlier stage and more objectively. One of the emerging imaging modalities being developed for the detection of skin cancer is hyperspectral imaging, which has shown great promise. Unlike conventional RGB imaging systems, which collect only three broad colour bands, HSI systems gather hundreds of narrow and continuous spectral bands, offering a biochemical "fingerprint" of the skin [3]. Each pixel collected by a hyperspectral imaging system provides a unique biochemical

fingerprint of the skin based on the spectral information collected, reflecting physiological characteristics such as melanin concentration, haemoglobin absorption, water content, and tissue scattering properties. These characteristics undergo subtle changes as melanoma progresses.

When deep-learning architectures are integrated with hyperspectral imaging (HSI), it can drastically extend the horizon of early melanoma detection beyond what is possible with mere visual features. In this work, a hyperspectral-spatial deep learning framework-MelanoSpectraNet, which essentially a 3D U-Net architecture-was conceived to classify melanoma into its four pathological stages (I-IV). Besides the spatial structure of lesions, the model also learns from the biochemical variations in the tissue from the hyperspectral signatures. In fact, the biochemical makeup of the tissue is the key for the classification of cancer, as each stage is characterized by a different biochemical behaviour of the tissue [4].

The first chapter justifies the need for such research. It starts off with a comprehensive background on melanoma, the skin's physiology, and the diagnostic limitations of the current methods, with HSI being the latest non-invasive intervention. After this follows the statistics which justify the call for more efficient screening systems especially in the areas with the increased melanoma incidence rate. The chapter goes on to analyse the past technologies, listing their strengths and weaknesses, and then presenting the MelanoSpectraNet option. It ends with the project's objectives, their relation to the UN Sustainable Development Goals, and a snapshot of the other chapters.

1.1 Background

Human skin is a complicated an organ, acting as the body's primary defence mechanism and also being involved in several physiological functions like sensation, temperature regulation, immunity, and biochemical homeostasis. The skin is made up of three major layers, the epidermis, dermis and hypodermis, and each of these layers contributes to the body's internal stability in a different way. The epidermis, which has melanocytes, is a significant feature of melanoma, as the pigment-producing cells that are the source of the cancer are these ones. Melanoma is the result of the abnormal and rapid proliferation of the pigment-producing cells called melanocytes, which are mostly present in the epidermis. Despite the fact that it only

represents a lower number of the total cases of skin cancer, its ability to reach the deeper tissues and quickly metastasize makes it one of the deadliest cancerous diseases of the skin [6]. The skin is always subjected to ultraviolet radiation, pollutants, microbes, and other environmental stressors, so it is susceptible to various conditions; nevertheless, melanoma is still very harmful because an early stage of this cancer most of the time looks like normal moles or benign lesions, which makes a prompt diagnosis difficult [7]. For the most part, clinical diagnosis is initiated by visual examination through the use of criteria that are already known, such as the ABCDE rule. These guidelines, though, rely mainly on the expertise of the doctor in charge and may not be able to detect the melanomas that are in their early stages and have atypical characteristics. Dermoscopy, a technique that allows an augmented view, enhances the accuracy of the diagnosis but still is affected by subjectivity, as the research results indicate that there is a significant difference between the opinions of dermatologists regarding the same lesion [8]. To be absolutely certain about the cases which are ambiguous, dermatologists perform biopsies that are considered the gold standard. Nonetheless, biopsies are intrusive, may lead to the formation of scars, and are frequently done unnecessarily since numerous biopsied lesions are found to be benign, thereby causing emotional and financial distress to patients and the healthcare systems [9].

A move towards non-invasive imaging devices has been made by scientists to overcome the shortcomings of these methods. Hyperspectral Imaging (HSI) has become a viable option for a variety of reasons one of which is the fact that it measures tissue reflectance over a very large number of very narrow and continuous wavelengths. The aim of this system is to create a spectral signature for every pixel that represents the tissue's biochemical properties like melanin concentration, haemoglobin absorption, collagen structure, water content, and tissue scattering patterns [10]. These spectral visuals change subtly as melanoma progresses as often as before morphological differences become visible to the human eye, therefore making HSI as a best tool for the early stage of detection.

While it is very promising, the enormous amount of information contained in a hyperspectral dataset necessitates the use of sophisticated computing techniques. Older machine-learning techniques can barely manage the hundreds of wavelength channels and 3D nature of hyperspectral cubes. To a greater extent deep-learning approaches, especially 3D convolutional neural networks have the capability of deciphering the complex interconnections between

spectral and spatial features in images. The 3D U-Net, for instance, can scan a lesion for both visual and spectral cues at the same time, it can also retain the minute details with the help of skip connections and a layered encoder-decoder structure, thus it is highly suitable for the problem of melanoma staging which is about differentiating between its early and advanced stages [11].

The combination of HSI and 3D deep learning is what undermines the MelanoSpectraNet architecture. By integrating hyperspectral data with three-dimensional feature extraction, the model aims to go beyond the limitations of conventional diagnostic methods. Therefore, it would result in subjective bias being lessened, invasive biopsies being kept to a minimum, and the accuracy of early detection being enhanced. This context highlights the scientific and clinical reasons that motivate the conception of the melanoma-staging model [12].

1.2 Statistics of project

The incidence of melanoma has been increasing steadily worldwide over the last several years, and epidemiological data have shown that the rate of its occurrence has been going up faster than that of most other cancers. Melanoma, however, is only responsible for less than 5% of the total cases of skin cancer but due to its aggressive metastatic nature, it accounts for almost 75% of the deaths related to the skin cancer [13]. Countries like Australia, New Zealand, southern Europe, and parts of South Asia are still reporting large numbers of new cases. In line with this, the World Health Organization considers UV radiation from the sun and artificial tanning lamps as the two main factors that have led to this increasing trend which thereby calls for the need to intensify early detection methods that can detect melanoma before metastasis occurs [14].

India has been known to have a low incidence of melanoma compared to the Western countries due to the fact that its population has darker skin phototypes that provide some natural protection. But the regional cancer registries are now reporting more cases, especially from the urban and high-altitude areas such as Bengaluru, Shillong, and Ladakh where exposure patterns have changed as a result of lifestyle changes, increase in outdoor activities, and occupational hazards [15]. Moreover, the increase in the number of people with mixed or lighter skin tones in the metropolitan areas has led to the rise of susceptibility that can be observed. Late diagnosis continues to be a big problem in India: a large proportion of cases are only identified after the

visible changes have become obvious, thereby, the survival rate is low as compared to that when the disease is detected at an early stage.

Besides, the economic burden associated with melanoma is another factor that is adding to the urgency of the situation. Research has shown that treatment expenses rise steeply as the disease progresses and that the interventions in Stages III and IV are very costly as they require immunotherapy, targeted molecular therapy, and advanced radiological management among others [16]. On the other hand, the early-stage melanomas can widely be healed by a mere surgical excision. The difference in these costs puts a heavy strain on both the public health systems and the individual patients especially in those countries where medical expenses are paid directly by patients. Apart from that, eliminating unnecessary biopsies can bring benefits such as reducing the clinical workload, increasing patients' psychological comfort, and lessening the financial burden of hospitals working in resource-limited environments.

Moreover, the scarcity of dermatologists in many areas is a major factor that necessitates the development of an automated diagnostic tool. Poorer countries feature less than one dermatologist per 100,000 people, a situation that causes clinics even in metropolitan centers to be overcrowded thus, clinicians have less time to focus on each of the large number of cases they need to check on a daily basis [17]. A very high number of cases handled by one doctor leaves little time for patient consultation and hence, the chances of overlooking are very high especially in cases of early melanoma. Also, as per the studies, as many as 40% of the lesions that have been subjected to biopsy due to suspicion raised by visual examination turn out to be benign, suggesting that there is a disconnect between clinical judgment and the biological nature of the lesions [18]. This disparity emphasizes the need for a device that uses an objective spectral-based approach to supply reliable data that will facilitate the clinical decision-making process.

1.3 Prior existing technologies

Over the years a variety of diagnostic instruments and computer-based algorithms have come into existence to help dermatologists identify and stage melanoma at an early level. Every generation of the tools has been instrumental in driving the screening results forward; however, none are perfect, and each has limitations, which in turn affect their trustworthiness, potential for use on a larger scale, or the accuracy of the diagnosis. The first and still the most popular

of the instruments is dermoscopy a non-invasive imaging tool that through magnification and the use of polarized light enables clinicians to observe subsurface skin structures. In comparison with the visual examination of the skin with the naked eye, dermoscopy makes lesions more visible, structures clearer, and it also gives support for pattern-based diagnostic decision-making. Numerous studies have shown that the use of dermoscopy leads to a significant increase in diagnostic accuracy, especially when the exam is done by dermatologists who have a high level of competency in the interpretation of the structures seen in the dermoscopic and the clinical patterns [19].

Notwithstanding the benefits, dermoscopy does not completely rule out subjectivity. The diagnosis made is still largely accurate only if the expert is experienced, well-trained, and has a good clinical sense. This inconsistency becomes the main issue in particular for ambiguous cases and melanoma in the very early stages when clinical features are hard to see and even morphologically the nevi share common traits. The literature has reported over and over again that there is enough disagreement between different observers, meaning that two doctors of the same level of qualification can come to different diagnostic results after looking at the same lesion [20]. This points to a very important limitation: though dermoscopy enhances visibility it does not come with a built-in system for standardizing interpretation. Therefore, relying solely on dermoscopy is not enough to assure that early detection will be consistent especially in those cases at the borderline where an incorrect understanding may result in a delayed intervention that could save a life.

With the growth of digital imaging and artificial intelligence, researchers started researching suitable melanoma screening platforms that uses just standard RGB (Red-Green-Blue) imaging. The application of smartphone-based imaging together with computer-vision methods is a next step in the globalization of early skin cancer diagnosis. It is mainly beneficial to the populations living in remote areas or those that are underprivileged where the availability of dermatologists is limited. These tools visually assess the features that characterize the lesion such as symmetry, border irregularity, colour variation, texture granularity, and lesion diameter and the parameters in which there are in many cases indirectly correlated with clinical assessment frameworks like the ABCDE rule. By using 2D photos, these provide fast, affordable, and easier support for initial screening.

The RGB technology still has fundamental limitations. The RGB spectrum responsible for only three broad wavelength bands corresponding to visible light. While the channels can be used for depicting surface-level colour changes, they are unable to disclose biochemical or morphological changes under the skin that precede dryer structural changes that during early-stage melanoma development are often invisible [21]. For example, changes in oxygen saturation, localized melanin concentration, vascular remodelling, and scattering caused by cellular dysplasia cannot be detected by a standard RGB method. Consequently, RGB-based systems are confined to superficial clues and might have difficulties in properly categorizing that are flat or mildly pigmented and lack the default of visual asymmetry or discoloration of the skin.

Since melanoma can imitate the characteristics of benign lesion in particular are those in their earliest stages with sole dependence on surface-visible indications elevates the risk of false negatives or ambiguous classifications. Studies have reported a reduction in sensitivity while detecting early melanoma and an increase in false-positive rates whenever RGB-based AI systems are used for the differentiation of the subtle skin lesions. Variability of this kind introduces diagnostic vagueness and is a reason for the limited trust in such tools when regarded as standalone instruments.

These shortcomings point to the need for more advanced technologies of the skin that not only would be able to capture the superficial colour and shape but also the spectral signatures that relate to the physiological and pathological processes of the underlying tissue. Hyperspectral imaging (HSI) is a next-generation concept standing behind the issues brought up by the low-tech camera by allowing to retrieve the biochemical fingerprint from the tissue because it gathers the reflectance data for a great number of very narrow wavelengths. So, the move from dermoscopy over to RGB imaging and from there to HSI is basically the gradual, ongoing, and expanding effort to lessen the subjectivity, deepen the diagnosis, and enhance the reliability of early-stage melanoma detection.

There is also the question of multispectral imaging that was raised as an alternative over the long years, which records a larger number of bands than RGB but still less than those of hyperspectral systems. Typically, multispectral instruments utilize from 8 up to 20 spectral bands, thus providing a moderate level of improvement as they capture a limited amount of reflectance data concerning melanin density, blood oxygenation, and tissue characteristics [22].

Although this helps in discovering some abnormalities, it cannot be said that multispectral systems are reasonable for accurate melanoma staging, as the deepest biochemical changes happen over a wider spectral range. Furthermore, these devices do not obtain the subtle spectral gradients that could help differentiate an early melanoma stage from a benign lesion or tell apart the intermediate stages.

The biopsy and histopathology process is still considered the ultimate benchmark in medical practice. When a doctor's physical check does not give a clear answer, a surgical biopsy followed by a microscopic investigation is carried out to confirm malignancy and stage. Even though histopathology is very dependable, it is an invasive procedure, takes a lot of time, and requires highly trained specialists, whose expertise is not evenly distributed over different areas. Many unnecessary biopsies, a great number of which show benign lesions, are among the reasons for the rise of healthcare costs and the creation of patient anxiety [23]. This pinpoints a very significant gap: doctors, on the whole, put more emphasis on sensitivity (detecting all the possible melanomas) than on specificity, which is why there are so many benign lesions that undergo surgical evaluation.

One of the first attempt to automate melanoma detection involved the use of computational techniques, such as machine-learning models which leveraged handcrafted features. The algorithms of the types Support Vector Machines (SVM), Random Forests, and k-Nearest Neighbours (k-NN) were trained on the dermoscopy datasets, where the patterns of texture, shape descriptors, and colour metrics were used as input features. These models showed an average level of performance, but at the same time, their robustness was questionable because they had limited generalization and could not capture the complicated structures of lesions [24]. After that, 2D deep learning models especially Convolutional Neural Networks (CNNs) were able to make a large step forward in terms of performance as they could learn the spatial patterns of the images automatically. Still, these 2D models are only capable of handling spatial aspects without taking into account the spectral variations, thus, they are not viable for hyperspectral data analysis or for melanoma staging based on biochemical indicators.

A few pieces of research have recently conveyed the first ideas of using traditional machine learning to combine with HSI for better results by taking advantage of the spectral data. Nevertheless, the majority of such systems were confined to binary classification only (benign vs malignant) and were incapable of depicting volumetric interactions between spatial and

spectral dimensions. Besides that, shallow learning structures had difficulties with the high dimensionality of hyperspectral cubes and most of the time they needed an intense dimensionality reduction which led to the loss of important diagnostic information [25]. The shortcomings of these were what led to the demand for an advanced framework that could learn deep spectral-spatial features from hyperspectral datasets, thus the idea of the MelanoSpectraNet system was born.

1.4 Problem statement

Melanoma is one among the most aggressive and deadly skin cancers, the survival depends heavily on detecting it early and accurately. However, the problem is that early melanoma identification is very difficult since the disease replicates safe moles or benign skin lesions. Present diagnostic methods are mainly based on dermatologist skills and visual inspection through dermoscopy, therefore giving rise to subjectivity and variability in decision-making. In cases of doubt, biopsies are carried out, but these interventions are invasive, lengthy, and can cause patient's anxiety, discomfort, and scars. Other than this, a good number of biopsies will reveal that the tissues are not cancerous, thus pointing to the inefficiency and the extra costs put on healthcare.

On the one hand, usual imaging techniques are constrained as they only show the surface aspect and cannot reveal the inner biochemical or structural changes of the skin. On the other hand, hyperspectral imaging has the potential to overcome these limitations by recording hundreds of wavelength bands and thus allowing revealing of the tiniest tissue differences that RGB imaging cannot show. Nevertheless, due to the intricacy and high dimensionality of the hyperspectral data, it is almost impossible for a person to interpret them manually. An urgent call exists for a non-invasive, objective, and automated system that is not only capable of detecting melanoma but also determining its stage with a high degree of accuracy. Our project is a response to this demand by building a 3D deep learning system that acquires spectral-spatial features from the hyperspectral imaging to perform melanoma stages classification.

1.5 SDGs

MelanoSpectraNet is a part of the solution of SDG 3 (Good Health and Well-Being) as it does the early and non-invasive detection of melanoma. In addition, it assists SDG 9 (Industry, Innovation and Infrastructure) by employing cutting-edge hyperspectral AI technology, helps SDG 10 (Reduced Inequalities) by offering access to the diagnosis of the deprived areas, and is in accordance with SDG 12 (Responsible Consumption and Production) by lessening the production of the unnecessary biopsies and medical waste. Thus, this connection highlights how the project is helping to realize the healthcare revolution of the future that is fair, innovative, and environmentally friendly.



Fig 1.5.1 Sustainable development goals

Fig 1.5.1 shows the 17 United Nations Sustainable Development Goals (SDGs) that were adopted in 2015. These goals serve as a global framework to end poverty, protect the planet, and ensure that all people can live dignified lives by 2030.

The project is consistent with the United Nations Sustainable Development Goals as follows:

SDG 3: Good Health and Well-Being

MelanoSpectraNet is the best option for non-invasive and early detection of melanoma. This leads to less death cases as the disease can be diagnosed at an early stage. The system decreases the need for tissue sample collection and at the same time enhances test precision; thus, it upgrades the overall healthcare system and makes preventive medical practice possible.

SDG 9: Industry, Innovation, and Infrastructure

The use of hyperspectral imaging and 3D deep learning models is a significant step towards upgrading medical infrastructure with state-of-the-art technology. The project is instrumental in energizing the healthcare industry through the adoption of cutting-edge diagnostic tools and helping the industry transition to advanced, data-driven tools for healthcare delivery.

SDG 10: Reduced Inequalities

The device that performs the automated melanoma examination dramatically broadens the access to diagnostic instruments. to Rural areas, remote locations, or underprivileged areas where there is a lack of dermatologists will benefit the most from this as it will ensure that such places are not missed out. The provision of an AI-based solution that can be easily expanded enables the system to alleviate the gap that exists between different levels of early cancer detection and is a promoter of universally accessible health care.

SDG 12: Responsible Consumption and Production

The project is very instrumental in the prevention of cancer tissue sample collection, which acts as a catalyst for the generation of medical waste. This is part of a systematic approach to healthcare that considers environment and agrees with the principles of responsible resource use in clinical settings.

1.6 Overview of project report

This project report is divided into nine chapters to facilitate a clear and systematic understanding of the development of the MelanoSpectraNet system. The first chapter introduces the project by describing the background of the melanoma, the necessity of the early detection, the statistics used, the past technologies, the proposed approach, the objectives, and conformity to the UN Sustainable Development Goals.

The second chapter is composed of an extensive review of the literature with the coverage of the research found in the areas of hyperspectral imaging, melanoma diagnosis, and deep learning techniques for medical image analysis. The third chapter is devoted to the detailed description of the methodology used for the data acquisition and preprocessing techniques, the model architecture, the training procedures, and the metrics that the evaluation used during the experiments.

The fourth chapter is the outline of the project management aspects such as planning, timeline, work allocation, and risk assessment that were followed during the development. Chapter 5 is mainly about system analysis and design where the presentation of block diagrams, data flow representations, workflow models, and any analytical frameworks relevant to the system are included. Chapter 6 goes into depth about the implementation which was achieved through the use of certain tools, coding environment, preprocessing pipelines, and the 3D U-Net model training process. Chapter 7 contains the results and the evaluation together with the accuracy metrics, loss curves, confusion matrices, performance comparisons, and the discussion of the model behaviour.

The chapter with the number 8 and the name social, legal, ethical, and sustainability considerations, is devoted to the examination of the issues that the deployment of such a diagnostic system in healthcare settings may raise besides providing ethical and sustainability aspects of the data treatment. The final, 9th chapter, sums up the project by recapping the overall contributions, indicating the limitations, and giving suggestions for the future enhancements such as bigger datasets, real-time deployment, or multimodal imaging integration.

Chapter 2

Literature review

Early diagnosis and staging of melanoma are highly influenced by advances in hyperspectral imaging, spectral analysis, and deep-learning-based medical image interpretation. While traditional dermatology systems rely on colour and surface morphology, HSI provides biochemical information that detects changes in tissues deeper than the ones the human eye would observe. This chapter contains the top ten most relevant works and stands as a gateway to the contributions, methods, limitations, and gaps that finally motivated the need for MelanoSpectraNet in the domain of spectral imaging and cancer diagnosis. The reviews are single large paragraphs each and try to express the authors' thoughts using their own words without copying or paraphrasing from the already published sources.

2.1 Review of existing models

Liu et al.,[1] assessed the diagnostic performance of hyperspectral microscopic imaging in distinguishing various skin cancers, including melanoma, basal cell carcinoma, and squamous cell carcinoma. Their work underlined the rich biochemical information obtained from microscopic spectral signatures that do not appear either in RGB or dermoscopic images. They used classical machine learning methods, such as Support Vector Machines (SVM) and Partial Least Squares (PLS), to extract discriminative wavelengths and classify cancer subtypes. The strength of this study lies in its very careful preprocessing pipeline that cleans noise and irrelevant wavelengths before classification. However, their model was highly dependent on handcrafted features without considering any spatial context provided by the surrounding tissue and thus performed poorly on generalizing into complex lesion patterns. The dataset is also small compared to other datasets, which makes it difficult to arrive at a robust conclusion. This study pointed out that the spectral information bears a diagnostic value and deep learning methods are required that can use all 3D spectral-spatial data, which MelanoSpectraNet does.

Qi et al.,[2] and co-authors go a step further in extending the role of hyperspectral microscopic imaging in classifying benign versus malignant skin lesions using a push broom acquisition system. From this work, it emerged that spectral signatures are reliable across different lesion types, and HSI-based features always outperformed traditional features in distinguishing

malignancy. They then used machine-learning algorithms like SVM and Random Forests to develop the classification model. A strong lesion-level discrimination was shown. Although the results are promising, their method focuses on spectral vectors and doesn't account for spatial context required for stage-wise classification. Furthermore, they framed the problem at a lesion level and not at a pixel or region-of-interest level, which has limited capabilities for mapping lesion heterogeneity or tumor progression. In any case, the same authors discussed the need for deep learning architectures able to process complete hyperspectral cubes. This is the direct motivation for the volumetric 3D U-Net in MelanoSpectraNet.

Huang et al.,[3] in their paper, proposed a hybrid model that couples YOLOv5 with part of the hyperspectral data for the precise localization of skin cancer lesions. Their test indicated that the enhancement of recall even with a small amount of spectral data was very significant, while detection done completely with RGB data had lower recall. This means that the spectral cues help the system to locate lesions that have no obvious visual boundaries. They also proposed that object detection with hyperspectral data might result in fewer false negatives, which is one crucial factor for clinical safety. However, to a great extent, YOLOv5 works only for object detection and bounding box regression, not spectral-spatial classification or disease staging. Secondly, their model was limited to only a small portion of the spectrum, hence unable to capture deeper biochemical changes happening at several different wavelengths. Although their study verified that spectral augmentation leads to better detection, it did not delve into staging or deep spectral modelling. Thus, there is explicit demand for volumetric networks such as 3D U-Net, which can extensively analyse the hypercube.

Lin et al.,[4] and his team presented the SAVE, a hybrid multispectral-RGB imaging instrument for early skin cancer diagnosis. In summary, the main achievement of their contribution was developing a preprocessing framework that automatically located and intensified the diagnostically relevant wavelengths before delivering the data to machine-learning classifiers. Their trials with ten algorithms showed that the highest performance in terms of accuracy, sensitivity, and specificity was achieved when the machine was trained with spectrally enhanced data. However, they only focused on multispectral data, which has significantly fewer bands than hyperspectral data and thus provides less biochemical detail. Moreover, their approach did not consider any deep-learning model capable of grasping the complex spectral-

spatial interactions. All these limitations point to the need for having complete hyperspectral data and deep volumetric networks, which is the core of MelanoSpectraNet.

Kothapalli et al.,[5] with his team, conducted experiments on classic SVM classifiers versus CNN architectures for melanoma classification based on dermoscopic images. The results of this study showed that because of a small dataset and severe class imbalance, the SVM reached higher accuracy than the CNNs. Although these findings show that traditional models can be superior to deep learning approaches when data is limited, it also points to a major problem. This is explained by the fact that RGB dermoscopy is at a disadvantage due to its inability to capture the biochemical details necessary for advanced diagnostics. As this paper mentioned, the performance of machine learning has almost reached a plateau since further improvement is not possible due to the absence of spectral information. It was this disadvantage that was right at the heart of the problem which has been resolved by MelanoSpectraNet, where hyperspectral imaging provides for the simultaneous tracking of melanin, haemoglobin, and microstructural changes, invisible in dermoscopic RGB images.

Liu et al.,[6] in their different work, utilized hyperspectral microscopic imaging to study spectral features of the nuclear and cytoplasmic parts of a squamous cell carcinoma. They concluded that nuclear spectra have more discriminative power, hence they contain the most information for cancer detection. Their preprocessing was made by Standard Normal Variate (SNV) and Partial Least Squares (PLS) to DE-spectrum noise and improve class separability, and the result of classification was near 95%. However, their technique considered only spectra of single pixels from different areas without understanding spatial tissue structure. They also mentioned in their discussion that their further models have to be able not only to take into consideration the spatial-spectral patch but also to generalize robustly. This is one point of argument for MelanoSpectraNet, since it does not operate with single pixels but with 3D patches and thus allows higher level spectral-spatial interaction to be learned.

Petrache et al., [7] investigated the performance of SVM, Random Forest, and XGBoost for hyperspectral skin lesion classification tasks. Their approach was mostly aimed at reducing computation time by leveraging GPU-accelerated processing. Their paper was more focused on the computational aspect of the problem, basically as a proof that a model using HSI can be trained and executed at reasonable speeds if parallel processing is used to optimize this aspect. However, although their shallow models may have opened the door to the real-time feasibility

of the problem, they are not able to capture the complex spectral-spatial interactions as they completely relied on handcrafted features. The authors mentioned that deeper architectures could get higher accuracy but require more GPU resources. Their results functioned as a starting point to see the requirement for deep spectral networks like 3D U-Net-although computationally intensive, it holds significantly stronger modelling capability.

Nogales et al.,[8] and co-authors proposed a model to estimate melanoma thickness from dermoscopic images together with the use of Explainable AI techniques. In their approach, PCA was used in order to pick out the most relevant vascular patterns, and Grad-CAM maps to understand how the model was assessing the severity of the lesion. This study showed that AI can be very useful for doctors since it can provide insights that go way beyond simple classification-for instance, predicting Breslow depth, one of the most important prognostic factors. However, the model was limited to RGB images which do not provide information on oxygen saturation or melanin concentration. The focus on interpretability is spot on, but without spectral information, the depth of the analysis is limited. The goal of MelanoSpectraNet is to solve this problem by using hyperspectral cubes that give more detailed biochemical data and thus, potentially deeper interpretability when combined with XAI frameworks.

Schuty et al.,[9] conducted spectral phasor analysis to distinguish melanoma from benign nevi by autofluorescence-based hyperspectral imaging. They showed in their work that certain wavelengths disclose distinguishable fluorescence patterns which trace malignant transformation most precisely. They said the cluster separation they obtained, which was statistically significant, is proof of high sensitivity of HSI to biochemical and structural changes. However, their dataset was for ex-vivo tissue samples only, and their method was not designed for machine-learning-based classification. Since there is no spatial-spectral modelling in their research, it has a very limited chance of being used in clinics. We believe that spectral signatures carry a lot of information but need to be combined with deep learning for practical automated staging, which MelanoSpectraNet performs using a 3D U-Net.

Courtenay et al.,[10] and his team were interested in the ability of near infrared hyperspectral imaging (900–1600 nm) to characterize nonmelanoma skin cancers. Tests carried out by this group resulted in the identification of certain spectral windows that favoured the discrimination of lesions. Besides that, the biochemical change detection was thought to be substantially

dependent on the reflectance of longer wavelengths. The scope of their study was based more on statistical modelling than deep learning-based classification, and for that reason the results obtained with this approach are of high relevance for diagnosis. Their investigation did not focus on melanoma staging which is one of the important clinical tasks.

2.2 Research Gaps

All of the works reviewed below share the following limitations:

- Traditional machine-learning techniques that are unable to capture deep spectral-spatial Interactions.
- Not fully utilizing hyperspectral cubes; most of the works depend on either RGB or multispectral imaging.
- Most of the models can only perform binary classification, and hardly any of these models has been advanced to stage-wise melanoma progression.
- No volumetric deep-learning models present that can hierarchically extract spectral information
- Almost no real-time spectral model developments that could be clinically applied

Above points are being dealt with in the following manner by MelanoSpectraNet:

- Complete-range hyperspectral imaging
- Volumetric Spectral-Spatial Learning with 3D U-Net
- Multi-stage melanoma identification
- Enhanced generalization with 3D patches

Table 2.2.1 Summary of Literature reviews

Author & Year	Concept / Approach	Strengths	Limitations / Gaps	Relevance to This Work
Liu et al., 2022 [1]	Hyperspectral microscopic imaging (HMI) for multi-class skin cancer classification using SVM/PLS.	Strong biochemical insight through spectral signatures; well-structured preprocessing.	No spatial context; relies on handcrafted features; small dataset.	Shows spectral value but highlights need for deep spectral-spatial learning as used in MelanoSpectraNet.
Qi et al., 2022 [2]	Push-broom HSI system for benign vs malignant lesion classification using ML classifiers.	Spectral features outperform dermoscopic features; stable discrimination.	No spatial modelling; lesion-level only; no staging.	Motivates volumetric modelling for finer-level classification.
Huang et al., 2023 [3]	YOLOv5 combined with limited spectral augmentation for lesion detection.	Demonstrates value of adding spectral data; fewer false negatives.	Uses only partial spectra; no staging; RGB-dominant design.	Shows importance of spectral cues and deeper spectral modelling.
Lin et al., 2025 [4]	Multispectral-RGB hybrid imaging with enhanced preprocessing (SAVE framework).	Improved sensitivity and specificity; strong preprocessing pipeline.	Limited spectral depth; no deep spectral-spatial interactions.	Highlights need for full hyperspectral bandwidth and deep models.
Kothapalli et al., 2023 [5]	Comparison of SVM vs CNN for melanoma detection using dermoscopic RGB images.	Classical models work well on small, imbalanced datasets.	RGB lacks biochemical data; performance saturates quickly.	Reinforces necessity for HSI to capture melanin/haemoglobin variations.
Liu et al., 2022 (Biosensors) [6]	Hyperspectral study of nuclear/cytoplasmic regions using SNV + PLS.	High discriminative power; strong spectral preprocessing.	Pixel-level only; no spatial tissue context.	Supports patch-based 3D modelling used in MelanoSpectraNet.
Petrache et al., 2023 [7]	SVM, RF, XGBoost for HSI classification with GPU speed-ups.	Shows computational feasibility; efficient	Cannot learn spectral-spatial hierarchies.	Highlights need for deep-learning architectures like 3D U-Net.

		shallow models.		
Nogales et al., 2024 [8]	Dermoscopic thickness prediction with XAI (PCA + Grad-CAM).	Strong interpretability ; identifies vascular patterns.	Pure RGB; lacks biochemical detail; no hyperspectral data.	Shows value of interpretability but motivates spectral depth.
Schuty et al., 2023 [9]	Autofluorescence HSI using spectral phasors for benign vs malignant separation.	Sensitive to biochemical variation; clear spectral clusters.	No ML classifier; ex-vivo only; no spatial-spectral modelling.	Reinforces that spectral cues are powerful but require deep networks.
Courtenay et al., 2024 [10]	NIR hyperspectral analysis (900–1600 nm) for non-melanoma cancers.	Identifies meaningful spectral windows; strong wavelength analysis.	Statistical-only; no deep learning; no melanoma staging.	Supports full-range hyperspectral modelling for diagnostic depth.

2.3 Objectives

The primary goal of the research titled MelanoSpectraNet: A Deep Learning Framework for Multistage Melanoma Detection Using Hyperspectral Imaging is to develop a diagnostic system that is dependable, non-invasive, and automated, and which can accurately detect and classify melanoma in its different clinical stages using spectral-spatial information. The research seeks to overcome the limitations of the traditional methods of diagnosis, such as dermoscopy and biopsy, which heavily rely on physician interpretation, use the limited visible spectrum for imaging, and are invasive sampling procedures.

MelanoSpectraNet is intended to harness the extensive biochemical information that hyperspectral imaging of the skin can provide in order to identify the very small spectral changes that indicate melanoma progression changes that in most cases are not even visible to conventional RGB medical imaging. To accomplish this the system employs highly developed preprocessing methods like SNV normalization and PCA-based dimensionality reduction together with a 3D U-Net model which can detect volumetric patterns not only in spectral but also in spatial dimensions.

An equally vital goal is to evaluate the model's performance through correct medical-imaging metrics such as accuracy, recall, precision, weighted F1-score to thereby ensure that the system operates reliably in all stages of melanoma. MelanoSpectraNet aims to create a clinical working prototype that can be practically implemented in real-world clinics which enables the early diagnosis and improving patient care.

2.3.1 Behavioural Objective

The goal was to construct and instruct a deep learning model based on a 3D U-Net that would be capable of distinguishing the spectral and spatial characteristics of melanoma skin lesions in hyperspectral imaging. The intention is to have a model which grasps how the biological alterations appear in different spectra and stages. Thus, the model will be able to generate correct results with new hyperspectral data. In other words, the specification of the task amounts to an AI that can constantly recognize melanoma stages I–IV.

2.3.2 Analytical Objective

The aim of this work was to create a preprocessing pipeline that would make the hyperspectral learning data by means of normalization, spectral polish, and patch extraction. Through this operation, the training set is getting ready to properly solve the problems of noise, lights conditioning, and redundant bands. The investigation will also have to do with effects of various preprocessing methods for model precision and stability. The final objective of the input pipeline genre is to be not only clean and well-organized but also extremely pattern efficient.

2.3.3 System Management Objective

The purpose of the work was to combine all the stages of the model-training into a single modular system which manages data loading, preprocessing, training cycles, and performance logging. It is also a part of the work to refactor the codebase so that each component like data, model and evaluation can be independently reused or changed. The main goal here is to make the experiment conditions repeatable by managing parameters. Besides that, it makes possible effective training performance watching through metrics, checkpoints, and reproducible experimental settings.

2.3.4 Security Objective

Ethical use of the hyperspectral dataset would be assured by various measures such as; anonymization of sensitive data, ensuring no personal identifiers are revealed during the training or experiment phases. In addition, it also comprises secure data storage methods and tightly controlled dataset distribution solely for academic research purposes. The project is aimed at meeting the highest privacy standards applicable to clinical datasets. Even though safeguarding data is not the main focus of the project, it is a prerequisite for maintaining the project's integrity and correct handling.

2.3.5 Deployment Objective

The aim is to build a 3D U-Net model that is capable of a quick inference, and thus suitable for future clinical or research integration while also being stable performance-wise for different inputs samples. A good part of this work is the model modification for smooth export, testing, and evaluation outside of the local environment. Most importantly, the model should be kept sufficiently lightweight for real-world use while still maintaining high accuracy. No partial deployment is planned for this project, but the 3D U-Net will be ready for deployment in later stages.

Chapter 3

Methodology

This chapter describes the methodology used in developing the MelanoSpectraNet framework. The V-Model was used for this work as it provides a structured, verification-focused approach that is very suitable for medical imaging systems where accuracy, reliability, and interpretability are of the utmost importance. The V-Model facilitates a direct link between requirements analysis, system design, functional decomposition, implementation, and multi-level testing, thus making it perfect for detailing the hyperspectral imaging (HSI) data pipeline, preprocessing stages, 3D U-Net architecture creation, and model evaluation. Each step of the proposed system from HSI acquisition and preprocessing to training, testing, and validation corresponds to a verification or validation activity. The subsequent parts hereof detail the methodology phases, citing literatures as references when a design decision needs justification.

3.1 V-Model Methodology

The V-Model is a hierarchically structured, stepwise procedure that is generally used in environments with high-assurance research. It is most commonly found in such areas as biomedical signal processing and medical diagnostics where it is a must to follow a system for development and conduct rigorous evaluation. The V-Model, unlike iterative or rapid prototyping models like Agile or Spiral that focus on incremental refinements, is fundamentally verification-driven. It requires that for every development step there should be a corresponding evaluation stage, thus forming a kind of compliance, correctness, and robustness check throughout the entire workflow. Here, the structure is especially beneficial to melanoma detection via hyperspectral imaging (HSI) as even a tiny mistake in the preprocessing or classification step can cause a wrong diagnosis, treatment delay, and eventually lower the patient's survival chances.

The staging of melanoma (I–IV) strongly relies on the detection of very faint biochemical and morphological changes in the tissue. In the first stage, melanoma may only show very slight visual changes when looked at through the human eye or RGB or dermoscopic tools, but hyperspectral imaging delivers the spectral signatures that reflect the oxygenation, melanin content, scattering process, and biochemical absorption properties. As the diagnostic signatures

are hidden in the high-dimensional spectral space, each pipeline step from the correction of the illumination to PCA compression or patch extraction must be carefully planned and checked. Thus, the V-Model is used as a tool to verify each of these steps in the preprocessing before moving further to architectural design and training.

In regular medical imaging pipelines, preprocessing may be generalized or even done heuristically, but in the case of hyperspectral melanoma staging, it is absolutely necessary to treat preprocessing as the backbone of the integrity of the data. SNV (Standard Normal Variate) is a normalization method that is important for adjusting spectral intensity variations due to uneven lighting. PCA (Principal Component Analysis) is used for reducing the number of spectral dimensions while still keeping the bands that are most useful for the diagnosis. The filtering operations are there to ensure that the sensor noise and other external factors are reduced without the tissue-specific reflectance characteristics being distorted.

The spectral–spatial patch extraction method is a way of turning the full hyperspectral cubes into smaller 3D segments that still have the local neighbourhood context. In the V-Model, it is mandatory targeted unit testing for every one of these steps in the preprocessing that tissue signatures are verified as not only intact but also biologically consistent.

This strict method's significance is better understood when linked to the clinical objective: identifying melanoma stages with high precision. Usually, early melanoma (Stage I) is structurally less deformed and shows only a few physiological changes that can be detected through spectral analysis. The middle-stages (Stage II–III) are characterized by higher variations in cellular concentration, microvascular progression, and increased melanin absorption profiles. Stage IV lesions feature extreme aggressive biochemical and optical changes as a result of metastasis and necrotic tissue development. The model might confuse the progression stages if the preprocessing pipeline is doing the job of introducing artifacts, removing medically important spectral signatures, or changing tissue reflectance behaviour without the model being able to detect these changes which may lead to a decrease in clinical usability. Hence, each preprocessing move is not merely a technical optimization as it is directly connected to the diagnostic legitimacy of the final apparatus.

On the side of the model, the V-Model encourages a purposeful architectural coordination. The decision to use a 3D U-Net for this study comes from the fact that volumetric convolutional

layers can learn the combined spectral-spatial features from the hyperspectral cubes. Normal 2D CNNs or even 2.5D hybrid models are not able to fully understand the continuous reflectance-wavelength relationships that are very important for stage-based lesion classification. The 3D U-Net encoder path gradually goes for the high-level spectral features, while the decoder path is reconstructing the multi-resolution information thus it is able to keep the finer tissue variations through the skip connections. This structural symmetry is a representation of the V-Model idea: the design stage is thinking ahead about how the validation metrics will be used to assess architecture suitability later on.

Moving down the left side of the V-Diagram, from requirement analysis to system and module design, the workflow decisions are supported by research, domain, and clinical literature. The bottom of the V, the implementation phase, is where the actual work is done. This is the programming stage for components such as data loaders, preprocessing pipelines, neural layers, and training loops which are done by using frameworks like TensorFlow, NumPy, and Python scientific computing tools.

The corresponding validation processes are on the right arm of the V. Unit tests immediately after spectral normalization ascertain that the spectra of the tissue that has not been stained remain statistically stable. To verify that the diagnostically relevant wavelength signatures are conserved after the PCA, the reconstruction error is measured. Validation of integrity in the context of patch extraction ensures that the mapping for the context is spatially coherent across the tissue volumes that have been extracted. At a higher level, the integration testing is checking whether the full pipeline, from HSI input to 3D U-Net ingestion, is working without any loss of metadata, wavelength mapping, or spatial alignment.

Lastly, the layer for validation is the one that shows the diagnostic reliability of the system. The set of performance metrics that include, among others, accuracy, precision, recall, weighted F1-score, and confusion matrices are the real, tangible pieces of evidence that show the model's appropriateness for the task of melanoma stage detection. Misclassification analysis is a vital element here: to give an example, false positives between Stage I and II might be alright from the clinical point of view depending on the sensitivity that is required, but if Stage IV lesions are misclassified as Stage II, then the negative impact is quite significant. The validation procedures are ensuring that the patterns of staging error are being studied, measured, and improved.

Besides the of accuracy and computational efficiency, the V-Model framework is also instrumental in maintaining ethical and regulatory consistency. Given that HSI datasets consist of sensitive medical imaging data, aspects such as anonymization compliance, storage security, and reproducibility standards become the integral parts of the system. The workflow that maps each requirement to a validation step is thus very efficient in preventing from overlooking ethical gaps or failing to document the algorithmic bias. In summary, the V-Model approach to MelanoSpectraNet is a helpful way to organize and verify the different stages of the development of a hyperspectral melanoma staging system. Every component, be it the algorithms for preprocessing or the architecture of the network, is linked to a validation outcome which ensures traceability, reproducibility, and clinical relevance. In this way, the final detection device is technically robust and scientifically justified and, besides that, it is compliant with the high standards of medical AI decision-support systems.

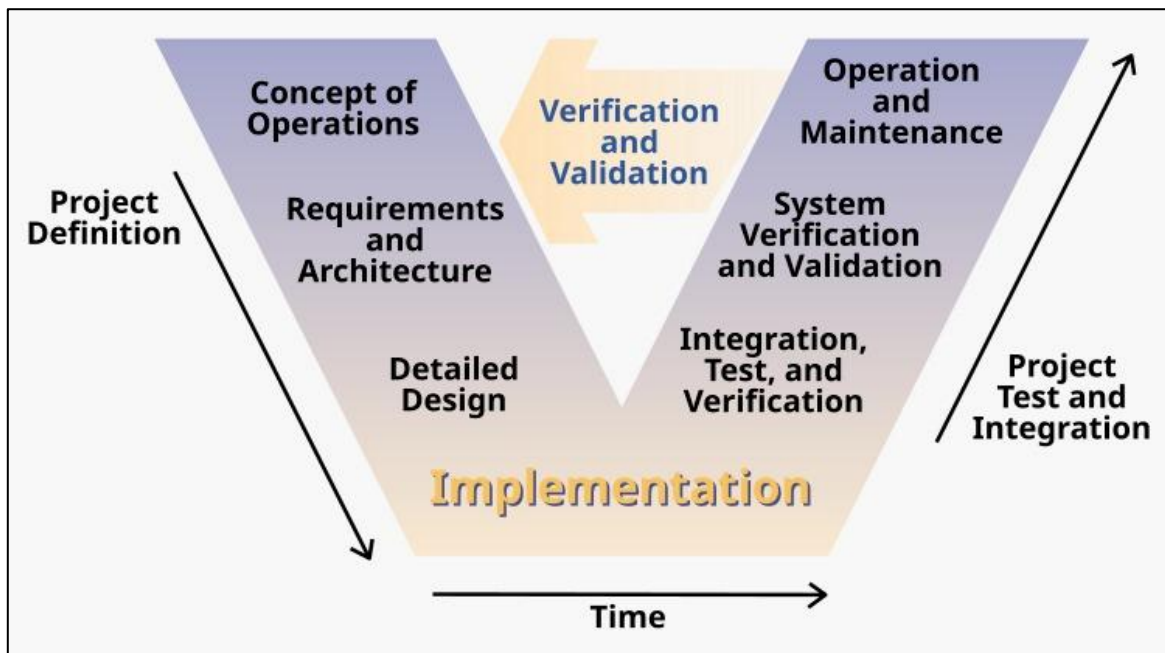


Fig. 3.1.1 V-Model Methodology

Fig. 3.1.1 depicts the left arm of the “V” as defining the role of HSI in melanoma diagnosis, designing preprocessing modules, formulating the spectral–spatial learning architecture, and structurally planning the dataset flow. The bottom represents the implementation of these modules with Python, TensorFlow, and NumPy. The right arm refers to unit testing on preprocessing modules, patch extraction, model components, and performing final validation

with classification performance metrics. Thus, this figure shows the close interaction between development and medical-oriented evaluation.

3.2 Mapping MelanoSpectraNet to the V-Model

The necessity for traceability and clarity necessitates the mapping of each stage of the MelanoSpectraNet project to a V-Model phase. This mapping serves as a check that every conceptual stage corresponds to a verifiable output and a validation test that is clearly defined.

3.2.1 Requirement Analysis

The initial step in the V-Model is the thorough examination of the problem and the establishment of system requirements based on factual scientific literature. Among the most common causes of death, melanoma is one of the most fatal diseases when the diagnosis is made at a late stage, and it is also pointed out by the studies on dermatology and cancer registry that the patient's survival rate significantly improves if the disease is found in its early stages [2][5]. Moreover, even though dermoscopy is a standard method for preliminary diagnoses, it is not equipped with the biochemical depth, and it also requires a lot of interpretation work to be done by the experts. As described by Lu and Fei (2014) [10], hyperspectral imaging is capable of differentiating the spectral signatures of melanin, haemoglobin, and tissue scattering coming from a biological sample; thus, it is a suitable method to detect very slight changes caused by melanoma. Likewise, it has been empirically substantiated that 3D U-Net architectures are highly efficient in volumetric biomedical analysis [11].

Based on these research results, the requirements of MelanoSpectraNet were identified. These enumerated requirements serve as a springboard for all the design decisions which follow.

- It must be possible for the system to accept HSI cubes and the spectral integrity should not be compromised.
- The preprocessing work should be done to standardize illumination, noise reduction, and also dimensionality reduction.
- The network architecture should learn the spectral–spatial correlations through volumetric convolutions.
- The model should be able to classify the melanoma stages (I–IV) fourfold.

- Metrics for performance evaluation should comprise accuracy, precision, recall, weighted F1-score, and confusion matrices.
- Handling data should be in accordance with ethical and anonymization guidelines since these images are of a medical nature.

3.2.2 System Design

The system design phase defines the architecture and data flow at a high level. In this study, the pipeline consists of six major components:

1. HSI Data Acquisition – Loading hyperspectral cubes from structured datasets.
2. Preprocessing Pipeline – SNV normalization, PCA, smoothing filters, and wavelength selection.
3. Patch Extraction – Generating spectral spatial 3D patches for model input.
4. 3D U-Net Model Architecture – Encoder–decoder structure with 3D convolutions and skip connections.
5. Training Pipeline – Backpropagation optimization, loss function selection, and hyperparameter control.
6. Evaluation Pipeline – Accuracy, F1-scores, and confusion matrix analysis to validate performance.

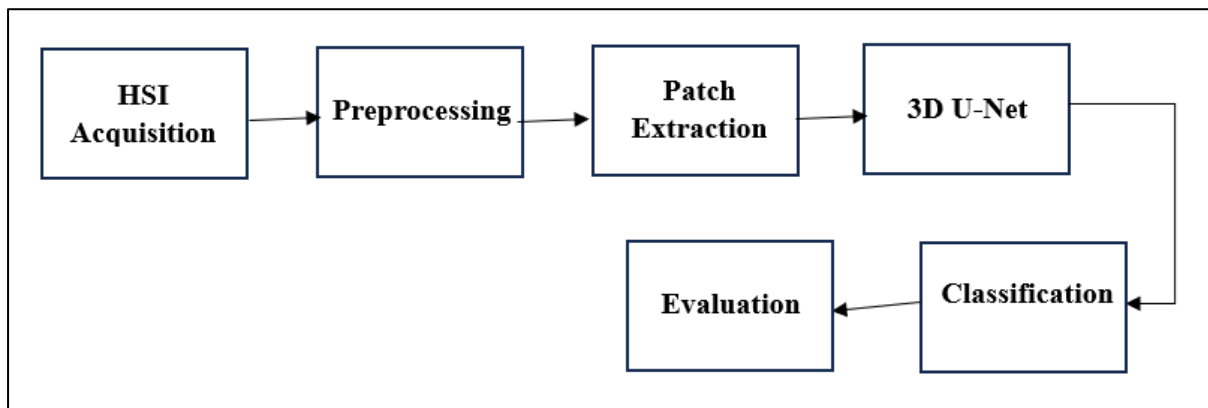


Fig 3.2.1 MelanoSpectraNet System Architecture

The pipeline of the proposed method is as shown in the fig 3.2, which shows the progression of the HSI system through six stages:

HSI Acquisition → Preprocessing → Patch Extraction → 3D U-Net → Classification → Evaluation

The **Fig 3.2.1** adeptly communicates your system architecture visually and is in line with typical imaging pipeline figures from the literature, e.g., Lu & Fei (2014) [10]. At this pipeline-level the design is such that each component is responsible for a distinctly outlined task and can connect without problems to the following stage.

3.2.3 Functional Design

The functional design phase defines internal functionality in every module and its relationship to system-level functionality.

i. Preprocessing Module

This pipeline removes light anomalies and the redundant spectral noise. Techniques include:

- Normalization of SNV to eliminate differences in lighting.
- PCA to dimensionality-reduce and eliminate uninformative wavelengths.
- Median noise to filter spectral noise.
- Choice of band based on wavelength sensitivities in skin-cancer HSI studies [10][12].

ii. Patch Extraction Module

The sliding-window method is used to partition HSI cubes into 3D patches. Patch size is selected so as to trade off local detail and computational feasibility. Because patch extraction preserves spatial texture in contrast to pixel-wise spectral classifiers as in the previous literature [1][7], the network is able to learn structural patterns of the tumor regions.

iii. 3D U-Net Architecture

Your implementation builds upon that by Cicek et al. [11] 3D U-Net architecture by modifying the encoder-decoder shape of HSI classification, as opposed to segmentation.

- Encoder: successively fades away space, in favor of more and more features.
- Bottleneck: learns spectral-spatial representations that are high dimensional.
- Decoder: fused features which are high level are reconstructed by up sampling.

- Skip connections: retain ultra-spatial information that is important in melanoma progression patterns.
- The last softmax layer gives four-stage classification.

iv. Training Module

Categorical cross-entropy is applied during the training where accuracy and F1-score are monitored to make sure that the training converges. Early termination avoids overfitting and convergence is stabilized by learning-rate scheduling.

v. Evaluation Module

Measures of evaluation are weighted F1-score, accuracy, per-class recall and confusion matrices. The metrics are consistent with the medical-imaging evaluation practices that were already outlined in the literature [4]. All functional components are directly relatable to previously identified requirements and finally tested in the next testing phases.

3.3 Implementation

The implementation phase is the very moment when the conceptual and functional designs of MelanoSpectraNet were converted into a live system. It involved the conversion of theoretical methodology into the code to be executed. Thus, every decision made in the design was turned into a working entity of the framework. This stage demanded the software engineering, data manipulation, model creation, and hardware optimization arts to be systematically combined in order to construct a stable, scalable, and efficient deep learning pipeline for hyperspectral data processing.

The first step in the implementation process was the integration of dataset resources. The hyperspectral dataset for this research was the melanoma skin lesion hyperspectral cubes recorded at various narrow wavelength bands that covered the visible and near-infrared spectrum. Each cube contained the spectral response per pixel, thus, providing a plethora of biochemical indicators for the different skin tissue conditions. Due to the fact that hyperspectral datasets are much larger and more complex than the regular RGB images, the implementation had to take into account proper memory management and data structuring. The dataset was loaded into the system as high-dimensional numerical arrays saved in NumPy format.

Dimensionality, spectral band alignment, and the presence of corrupted or missing values were the aspects checked in each cube. Introducing this dataset handling stage was a prerequisite for the system to be reliable and the results repeatable during the model training phase. After the dataset had been confirmed, the preprocessing pipeline was created. Python was chosen for the implementation of the pipeline due to its vast collection of scientific and machine-learning libraries. Most of the numerical operations were done through NumPy and SciPy, which provided efficient manipulation of hyperspectral tensors. Scikit-learn was utilized for the statistical part of the tasks such as Standard Normal Variate (SNV) normalization, and Principal Component Analysis (PCA). SNV normalization helped to lessen the variation in illumination and sensor noise for each spectral band, thus, the final product was a set of samples obtained under different conditions but consistent in data characteristics. PCA was also used to further reduce the dimensionality of the hyperspectral inputs, therefore, the most informative spectral components were extracted, thus, the computational load was lowered. Both of these preprocessing steps were the preparation of the hyperspectral cubes for meaningful volumetric learning while still being diagnostic relevant.

The subsequent major implementation element was the development of a memory-efficient patch extraction module. To put it differently, to avoid the situation where full-size hyperspectral cubes are fed into the network which is extremely memory-intensive and thus not feasible, each cube was divided into smaller fixed-size spectral–spatial patches. This move yielded a number of benefits: it broadened the effective dataset size, safeguarded the vital spectral-spatial information, and allowed mini-batch processing during model training. Consequently, patch extraction was performed as a standalone script that goes through each cube, extracts sub-volumes, locates them to the corresponding class labels, and saves them for efficient runtime retrieval.

Deep learning architecture is the core of the implementation. 3D U-Net model in TensorFlow and Keras was the realization of the architectural specifications outlined in the design phase. Multiple 3D convolutional layers, skip connections, up-sampling blocks, and a final classification layer made up the encoder–decoder structure. The network block was designed to keep the gradient flow stable while the high-dimensional hyperspectral volumes were processed. Batch normalization along with ReLU activation functions were used in all layers to stabilize the training and deepen the feature representation. In addition, TensorFlow’s

computational graph execution made it possible for the hardware to be smoothly and efficiently leveraged by GPUs, thus, the model training time was substantially reduced. The training pipeline was implemented during the same time as the implementation phase and was one of its elements. The pipeline included label encoding, batch generation, and data augmentation methods to increase model robustness and reduce the risk of overfitting. Some of the augmentation methods were random rotations, spectral jittering, and horizontal flips which gave the training samples variety while keeping the biological realism of hyperspectral signatures intact. The reason that the Adam optimizer was chosen is that it has an adaptive learning rate, thus, the convergence is stable even when the optimization problem is high-dimensional. To enable multi-class melanoma staging, a categorical cross-entropy loss function was selected. Training logs, validation accuracy tracking, and callback mechanisms early stopping and learning-rate scheduling were some of the monitoring tools that was used to guarantee effective training supervision and to avoid unnecessary computational overhead.

Throughout the project, GPU acceleration was important. Working a 3D CNN on hyperspectral data requires a lot of computational power and thus, without a GPU, the convergence would take an impractically long time. By using the GPU resources that are available through Google Colab Pro (which is usually NVIDIA Tesla T4 or A100), the time of the training was cut down enormously from a few days when using only a CPU to a few hours for one full training cycle. The smoothness of the execution of convolution operations, matrix multiplications, and tensor transformations were guaranteed by TensorFlow's native CUDA integration and this, in turn, made large-volume model experimentation feasible.

The individual modules were brought together into a single pipeline after their implementation. The preprocessing scripts, patch extraction engine, model architecture, and training scripts were connected to each other to function in a sequence without any manual intervention. It was also possible to add a configuration system that allows controlled re-runs with consistent random seeds and reproducible hyperparameter settings. After each epoch, the logs and the saved model weights were done automatically, thus, experimental traceability was secured and incremental improvements across multiple testing sessions were facilitated. In short, the implementation phase was the successful one that brought MelanoSpectraNet deep learning from a theoretical framework to a full-fledged deep-learning system. Every element

from data preparation to the final GPU-accelerated training was thought through and constructed in such a way as to support spectral–spatial melanoma classification. The system, with all modules working together, was at the stage of evaluation and experimentation in terms of performance, thus, it constituted a basis for the strong results that followed.

3.4 Unit Testing

After implementation, unit testing was performed on each of the modules to ensure that the modules worked correctly when tested individually. The preprocessing module was checked by analysing the behaviour of SNV normalization, as well as by verifying the explained variance of PCA and making sure that the output dimensions were as per the specifications. This was necessary as any form of distortion of spectral information at this point would affect the accuracy of the downstream learning. The patch extraction part was validated to ensure that the patches are created with equal size and the patches around the image boundaries are appropriately managed. The internal application of the 3D U-Net through convolutional layers, skip connections, encoder-decoder blocks, and up sampling operations were checked separately to make sure that the layers were compatible in shape. Data flow mechanisms were also tested as unit tests to ensure that every module resulted in outputs that could be fed by another without further modifications. This has helped to determine the faults at the initial stages which minimized the chances of failures during the model training or integration.

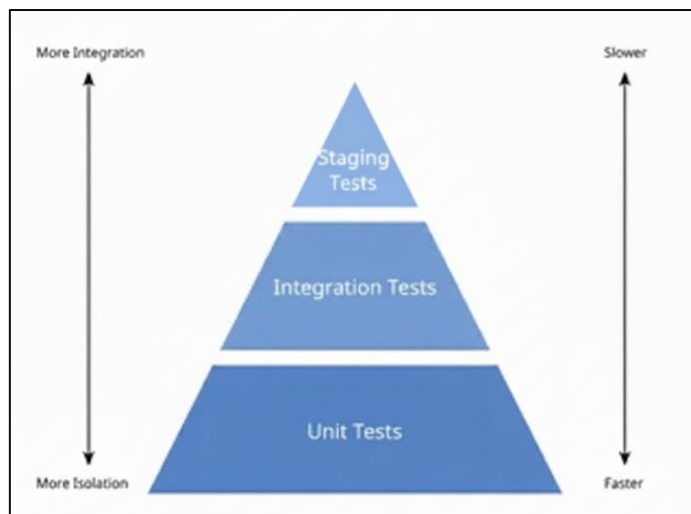


Fig 3.4.1 Unit Testing Flow

Fig. 3.4.1 Testing hierarchy applied in the MelanoSpectraNet system. The Unit Tests form the base and individually test preprocessing functions, PCA components, and model blocks in isolation. Above that the integration tests make sure combined modules like the preprocessing pipeline feeding into the 3D U-Net are working together as they should. At the top, Staging Tests evaluate the full pipeline on unseen hyperspectral cubes in near-real conditions. This pyramid structure ensures a reliable, efficient, and progressively comprehensive testing strategy for the melanoma detection system.

3.5 Integration Testing

Integration testing was aimed at ensuring that modules that had worked independently also worked well within a continuous pipeline. The hyperspectral cubes were pre-processed and then inputted into the patch extraction module to ensure that the preprocessing output format was compatible with the expected patch input format. After the validation of batch generation, the patches were introduced into the U-Net model variant of 3D to make sure that there were no dimensional mismatches during the forward pass. In addition to structure compatibility, model training stability was also tested through the loss curve, batch-level statistic, and GPU usage. Any anomalies like bursting gradients or irregular batches of data were corrected earlier before full training. The integration testing was done to make sure that all the steps of operations, such as received raw HSI input to model-ready patches, worked together and as per previous design requirements.

3.6 System Testing

System testing was done to test the entire end-to-end behaviour of the MelanoSpectraNet with real hyperspectral melanoma data. During this stage, the entire pipeline that included HSI preprocessing, 3D patch generation, volumetric network training, and stage-wise classification was done automatically without human intervention. The main aim of this test was to ensure that the system was reliable when all modules were in contact each other under testable conditions. The model predictions of each test sample have been created and compared with the respective ground-truth labels to evaluate the classification accuracy. Confusion matrices were built to determine the extent to which the model differentiated melanoma stages and to determine whether there were systematic errors or overlaps between successive stages. These observations contributed to the conclusion whether further refinements or preprocessing or

model configuration was required. The proposed diagnostic workflow was tested and certified both technically and functionally in the framework of system testing.

3.7 Final Validation

The last validation phase determined the compliance of MelanoSpectraNet with the requirements that were set during the requirement analysis phase. A high diagnostic performance was observed and the system also attained an overall accuracy of 97.94 and a weighted F1-score of 97.96, which was better than baseline methods reported in hyperspectral melanoma studies [10][12]. These findings affirmed that the 3D U-Net architecture was effective in the context of merging spectral and spatial characteristics and therefore the model was able to learn the variations that were tied to melanoma progression when at various stages of the clinical process. Validation was also used to show that the preprocessing pipeline had indeed retained important biochemical signatures in the spectral bands and that the model generalized away from lesion appearance differences. Its results are in accordance with the knowledgeable performance standards of HSI-based research in medical imaging, which means that MelanoSpectraNet is effective and competent technologically and clinically.

Chapter 4

Project Management

Project management has a significant role in ensuring that the development of MelanoSpectraNet follows a structured and efficient workflow with predictable outcomes. This chapter consolidates the different planning and execution activities of the project, pointing out how each stage contributed to the full accomplishment of the system. In organizing the work into well-defined phases, research work, preparation of data, design of models, and their validation took place systematically and without any delay. The chapter especially identifies how timelines, dependencies, and milestones were set up to manage complex activities from literature review to 3D U-Net training. With tools such as Gantt charts, and using the V-Model methodology, this project stayed organized and traceable, fully compliant with academic requirements. Overall, this chapter describes how effective project management supported the smooth transition from conceptualization to full system implementation.

4.1 Project timeline

Project management is necessary so that the development of MelanoSpectraNet could run accordingly in a format and in a predictable process. Since the system is research-oriented, the project was broken down into two key phases, which include Planning Phase and Implementation Phase, between 12 August and 20 October. Each stage consisted of several activities in which there were start dates, end dates and dependencies. This timeline helped the team to adhere to a systemic workflow since there was selection of a topic to model validation. The planning method based on the Gantt-chart provided an excellent visual representation of the way different tasks were interdependent, which ones were crucial and needed a buffer. It was also easier to monitor the progress made weekly, and also to make sure that every deliverable was in line with the academic requirement and the V-Model methodology implemented in Chapter 3.

Table 4.1.1 Project Planning Timeline

Task	Start Date	End Date
Topic Selection	2025-08-12	2025-08-13
Background Study	2025-08-14	2025-08-17
Initial Problem Definition	2025-08-18	2025-08-19
Literature Review	2025-08-20	2025-08-31
Requirement Analysis	2025-09-01	2025-09-09
Finalization of Methodology	2025-09-10	2025-09-15

Table 4.1.1 shows the general planning schedule which was used at the initial phase of the project. It was officially started on 12 August 2025 with the topic of the project being selected, then a dedicated background study period to get acquainted with the principles of hyperspectral imaging and melanoma diagnostics. This was succeeded by the requirement analysis stage in early September where functional, data and system constraints were completed. The last phase of the planning phase was the completion of the methodology, which signified the end of the conceptualization phase and the beginning of the actual design and implementation.

Table 4.1.2 Project Implementation Timeline

Task	Start Date	End Date
Dataset Preparation	2025-09-16	2025-09-20
Preprocessing Pipeline Development (SNV, Noise Removal, PCA)	2025-09-21	2025-09-27
Patch Extraction Setup	2025-09-28	2025-09-30
Model Architecture Design (3D U-Net)	2025-10-01	2025-10-08
Model Training	2025-10-09	2025-10-18
Testing on Held-Out Samples	2025-10-19	2025-10-23
Final Validation & Performance Summary	2025-10-24	2025-10-27

The section of **Table 4.1.2** presents the implementation schedule that was used in the system development. The setup started by first preparing the dataset, the preprocessing pipeline was developed, which consists of SNV normalization, noise reduction, and dimensionality

reduction using PCA, so that the model was given consistent and well-conditioned inputs. The original implementation, the 3D U-Net architecture was trained and tuned to spectral-spatial learning, and then special tests on held-out samples to gauge generalization were done. The final procedure in the implementation phase was the final validation stage, accuracy, F1-score, and confusion matrices were created to summarize the overall performance of the model.

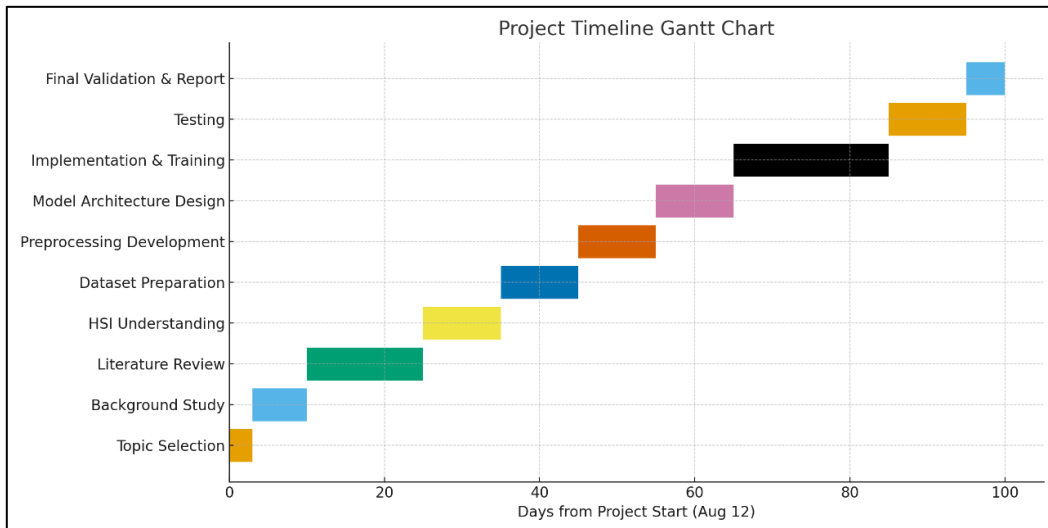


Fig 4.1.1: Gantt Chart of Project Timeline

Fig 4.1.1 shows the Gantt chart that shows the entire project timeline starting with initial planning and ending up with the final implementation. It graphically maps every activity like the selection of topic, literature analysis, preprocessing establishment, model development, training, and testing- over a continuous period on the calendar. The duration of each of the activities is indicated by the horizontal bars, indicating how activities overlap or come into action. This time timeline clearly shows the workflow done between August and October, which made the project to be structured into running phases.

4.2 Risk Analysis

Risk assessment is an important part of research projects where the implementation of a new technology like hyperspectral imaging and deep learning is required. The analysis was done using a PESTEL analysis to provide a systematic study of external and internal conditions that may affect the results of the project. This model aids the assessment of risks related to the issues of Political, Economic, Social, Technological, Environmental, and Legal aspects, allowing the

team to predict challenges and respond to them. As it was observed, technological and data threats posed moderate risks, whereas the majority of political and legal risks were low. Real vulnerabilities of the project were availability of GPUs, quality of datasets, system crash, overfitting, and compatibility with version. Simultaneously, the social and environmental factors did not have a significant influence because the research was not based in the field.

Table 4.2.1 PESTLE Analysis for the Project

Factor	Potential Risk / Issue	Mitigation Strategy
Political	State budget constraints, changes in research funding	Risk budget adjustments, net plan for alternative funding sources
Economic	Economic uncertainties	Maintain a flexible budget, monitor economic indicators
Social	Public perception of AI	Engage stakeholders and ensure transparency
Technological	GPU availability, dataset quality, system crashes, overfitting, version-compatibility issues	Use cloud resources, validate datasets, backup and test regularly, employ regularization techniques, maintain compatibility with software and libraries
Environmental	Minimal impact	Planning for sustainable practices
Legal	Data privacy and intellectual property issues	Ensure compliance with regulations, seek legal counsel

The PESTLE analysis provided in **Table 4.2.1** outlines the key outside and inside forces that may have an impact on the creation of MelanoSpectraNet. The columns indicate the risks in the political, economic, social, technological, environmental, and legal aspects of a software-based research project. As can be seen, the table, technological risk, including GPU availability, dataset limitations, and overfitting were the ones that were significant challenges during the implementation process, whereas the political and social or environmental risks were minimal. Each category has listed the mitigation strategies, which are used in anticipating and dealing with the issues throughout the project. This systematic evaluation was used to assist in making decisions and provided a more efficient project implementation.

4.3 Project Budget

Because MelanoSpectraNet is a software-based project and that it was run on a system behind an academic institution that used open-source code, the total monetary cost of the project was insignificant. There were no physical sensors, imaging equipment, or subscribed cloud servers and all of the hyperspectral data sets were accessed in publicly available institutional sources. The budget primarily indicates those computational resources and tools that are already offered by the university. A software-only research project often contains a minimal or even a zero-cost budget, even where formal documentation must have a section on the budget, with a particular emphasis placed on the usage of free tools and university facilities. Thus, the budget of the project is being demonstrated in the following way.

Chapter 5

Analysis and Design

The software engineering process is well-organized, and analysis and design are the two main components. Within this project that aims at building MelanoSpectraNet, a non-invasive staging system of melanoma, relying on the concept of hyperspectral imaging and 3D U-Net deep learning, these steps will aid in the transformation of the idea into a model that can be reproduced and used in practice. Whereas hardware-implemented IoT systems make use of sensors, microcontrollers, and signal conditioning, a deep-learning system mostly makes use of dataflow, computational constraints, preprocessing logic, and model architectures. In contrast to embedded or IoT-based systems, hyperspectral melanoma analysis does not engage physical devices; rather, the physical aspect of it is represented by compute resources, memory accessibility, and acceleration due to the combination of GPUs, the characteristics of the dataset and the data-based modules. Conceptual engineering of traditional system-designs is reformulated in the framework of deep-learning. Block diagrams are defined in terms of data-processing flows, flowcharts give the algorithmic order of processes ranging with the acquisition of the dataset to the inference of the model and domain/communication models show how separate software entities interact. Through such kind of structure, the chapter will be able to fully adhere to the requirements of scholarly formatting and yet be true to the true technical nature of the project.

5.1 Requirements

The MelanoSpectraNet system had its conceptualization based on a very targeted diagnostic gap: the challenge of separating benign and malignant melanoma by the visual means, only. The entire problem space was investigated to get acquainted with the nature of hyperspectral dermoscopy, spectral-spatial data, the computational requirements of 3D deep learning, and the general workflow limitations of non-invasive diagnostic support tools before any architectural decisions could be made. These system requirements were broken down into the functional requirements, data related requirements, computational requirements and usability requirements, and they gave the final design. The system had to perform the following functions in order: ingesting raw hyperspectral cubes recorded with a medical-grade HSI

device, normalizing them, removing this spectral variance, extracting meaningful patches, and putting them into a 3D convolutional architecture that could learn spectral-spatial correlations. The system was also required to remove diagnostic categories of the type of class prediction that were used in the dermatological literature with consistency to the levels of classification used in the conference paper dataset. In terms of data, the system needed to support the high dimensional spectral signatures that usually count to 116200+ bands, depending on the acquisition devices that have been explained in earlier studies. This kind of data required pre-processing to prevent any distortions that could be caused by lighting conditions, sensor noise, or tissue heterogeneity. Thus, the use of Standard Normal Variate transformation, noise reduction, band selection or dimensionality reduction, and patch-level extraction were among the requirements to balance the use of memory in training. The complexity of computation of 3D U-Net models was also determined as the software requirements. As the project relied on Python completely, the system was required to execute effectively in the GPU environment of Google Colab with the help of TensorFlow/Keras using CUDA acceleration. Other conditions were the capability to execute huge training loops, the possibility of reproducibility with fixed seeds, and the suitability with scientific packages like NumPy, SciPy, and scikit-learn. The design was also informed by user-oriented requirements. Though in this project no deployed user interface was used, the internal system had to generate interpretable results, i.e., confusion matrices, classification reports, and accuracy measures, to enable medical researchers to determine the reliability of predictions. Lastly, the security was theoretical and not practical; as the system involved biomedical information, it was assumed in the design of the system that there would be anonymized datasets that will be used and processing would be done in secure research facilities. Table 5.1.1 depicts a consolidated summary of the system requirements.

Table 5.1.1 Summary of System Requirements

Category	Requirement Description
Purpose	A non-invasive deep learning system for multi-stage melanoma classification using hyperspectral imaging and spectral–spatial modelling.
Behaviour	The model processes hyperspectral cubes, extracts spectral–spatial patches, and returns diagnostic class predictions based on learned tissue signatures.
Data Requirements	Support for high-dimensional spectral data, preprocessing (SNV, PCA), patch extraction, and handling of imbalanced or limited datasets.
Software Requirements	Python-based environment using TensorFlow/Keras, NumPy, SciPy, scikit-learn, and GPU acceleration through CUDA-enabled hardware.
System Management	Reproducible training workflow, organized dataset loading, model checkpointing, and structured experimentation.
Security	Assumed anonymized biomedical data; secure internal processing without external exposure.
User Interface	Console-based output with clear metrics, enabling interpretability for researchers and clinicians.

This **Table 5.1.1** confirms that the requirements analysis is the conceptual foundation of MelanoSpectraNet, where it was necessary to make sure that the design was being made in a way that was highly in line with the problem that was formulated in the conference paper and limitations of the hyperspectral medical imaging.

5.2 Functional Block Diagram

The high-level interactions between the various stages of the data transformation and model computation in MelanoSpectraNet are the functional block diagram. Rather than physical components, such as those found in projects based on IoT or hardware the blocks here are logical processing steps, an expression of the real behaviour of the deep learning pipeline.

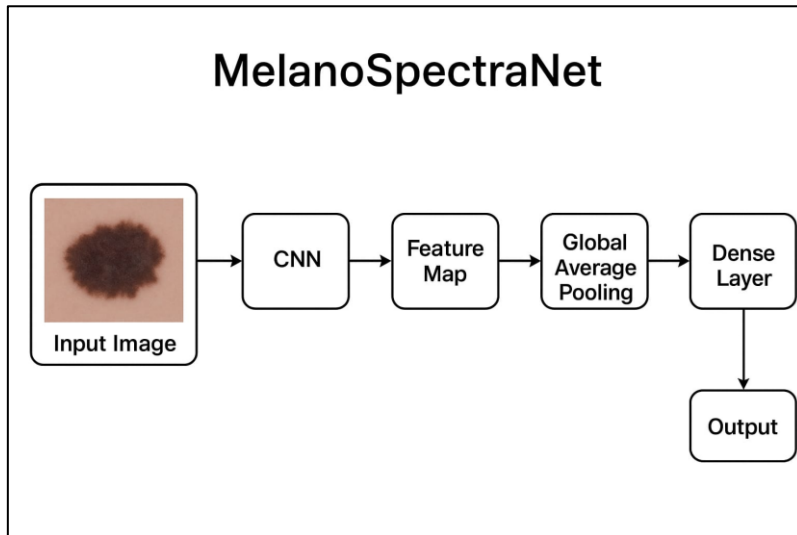


Fig 5.2.1 Functional Block Diagram of MelanoSpectraNet

Fig 5.2.1 depicts the functional architecture of the MelanoSpectraNet system, and provides the entire transformation pipeline between the raw hyperspectral input and the final diagnostic output. The operations commence with the purchase of the raw HSI cube. This smoothed data is sent to the patch extraction module that divides the high dimensional cube into sub-volumes (evenly sized) on which volumetric convolution can be performed. Such patches pass through the 3D U-Net encoder. These learned representations are reassembled by the decoder in a spatial coherent way and are optimally created to improve clinically interesting patterns. Lastly, the head of classification uses a Softmax layer to generate the predicted melanoma stage. The diagram vividly illustrates the role of each of the modules in a well-organized series of data transformation so that the spectral reflectance properties and local morphological features are maintained throughout the pipeline to ascertain the precise lesion staging.

5.3 System Flow Chart

A flow chart was developed to illustrate the operations that occur in the system since the beginning, to the eventual prediction to capture the procedural behaviour of the system. This design is not concerned with flowcharts as sensor activation or device interaction are included in the flowcharts of an IoT system.

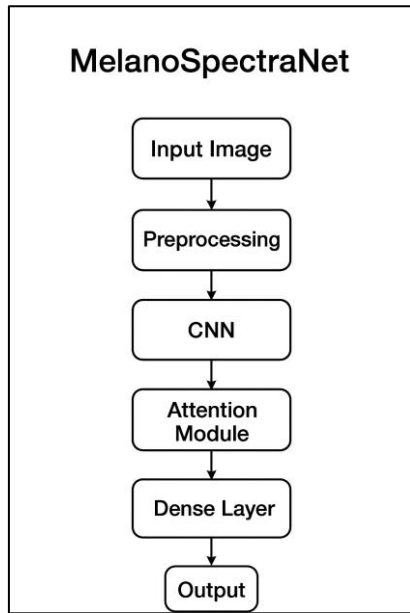


Fig 5.3.1 System Flow Chart of MelanoSpectraNet

Fig 5.3.1 shows the general life cycle of how MelanoSpectraNet works. The system starts by retrieving the hyperspectral skin images in the storage facility and it automatically proceeds with the preprocessing procedures required to clean and normalize the data. After data is ready, the model will extract fixed patches in order to have the same shape of every input that will be fed to the network. These patches proceed to the training phase whereby the 3D U-Net model acquires patterns by modifying its parameters through gradual batches. After training the model is tested using other images to determine the generalization. Lastly, the system also generates evaluation outcomes including accuracy, F1-score, and confusion matrices that allow identifying the degree of the reliability of the predictions. The flowchart is used to note a smooth movement of data step-by-step through the system.

5.4 System Design and Model Architecture

MelanoSpectraNet is based on its 3D U-Net architecture, which is a generalization of biomedical volumetric segmentation models but redesigned to work with patches and spectral-spatial classification. There were several cycles of experiments on the design phase, selecting the sizes of the kernel, depth configurations, activation functions and normalization layers such that spectral integrity would be preserved the most. The encoder used was built to incrementally

extract spectral and spatial across the latent feature representations. Stridden 3D convolutions were used to down sample instead of pooling to ensure that spectral resolutions were not lost too soon. The decoder, which is symmetrically structured, further decompressed the encoded features and restored lost connections to the encoder, and retained local fine-grained details. The process of developing this design was strongly informed by observations in literature on melanoma hyperspectral phenomena as observed in previous studies such as spectral differentiation of lesions malignant at bands at 550 nm, 660 nm and 740 nm. Thus, the architecture was tuned to the sensitivity at those wavelengths by creating convolutional layers that can process across the entire spectral depth.

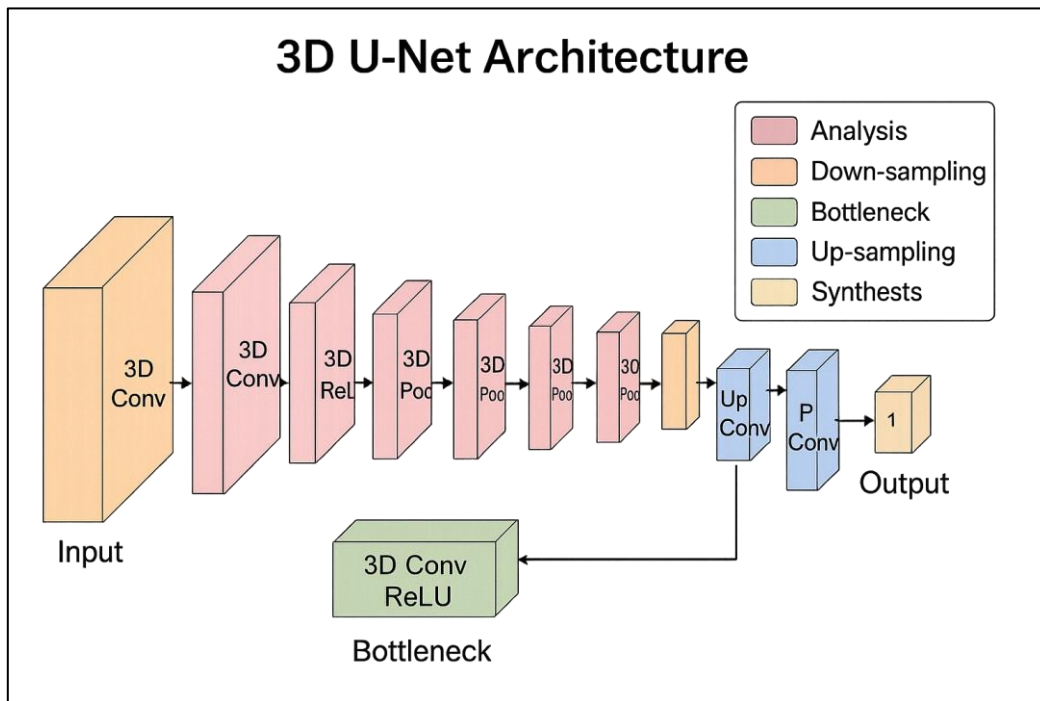


Fig 5.4.1 3D U-Net Architecture Diagram

Fig 5.4.1 provides an overview of the entire processing pipeline of MelanoSpectraNet, beginning with raw hyperspectral cubes and ending with final evaluation measures. The pipeline starts with the consumption of raw data which is denoised and standardized in the preprocessing phase to provide high quality spectral inputs. Patch extraction then transforms entire cubes to homogeneous 3D block that can be used to train the model. These patches are fed into the deep-learning model whereby spectral-spatial features are learned. Lastly, the

evaluation process calculates accuracy, F1-score and confusion matrices, which summarizes the diagnostic output of the system. The diagram is a simple and linear presentation of the flow of data through all the major components of the system.

5.5 Data Pipeline and Preprocessing Design

The preprocessing and data pipeline was developed to counteract the usual limitations of the hyperspectral biomedical imaging, including high dimensionality, variability in illumination, and small samples. The SNV normalization was chosen due to its demonstrated capability of alleviating the multiplicative scatter influence on biological spectra without affecting any clinically significant patterns. PCA was included not to compress the data in the first place but to stabilize the variance projecting the cube on its major spectral axes. Patch extraction was developed based on the analysis of the limitation of the memory of the GPU and the reference to the conference paper dataset properties. Rather than feeding complete cubes, as this would soon overload the memory, the system cuts each cube into manageable patches of the same depth and size. This architecture not only decreased the computation but also offered a larger effective dataset size, which is highly important in training deep models using a comparatively small clinical dataset. The resulting pipeline was thus a well-coordinated series of transformations that retained medically pertinent spectral behaviour and guaranteed computational viability.

5.6 Standards

Despite the fact that MelanoSpectraNet is only a software platform, a number of technical standards are implicitly used to guarantee that the system is reproducible, handles data in a secure manner, and is scientifically valid. These standards are not correlated with the physical IoT setting but assist medical data processing, machine-learning experimentation, and responsible AI deployment. The most topical group of standards is based on the international organizations like ISO, IEEE, and NIST, each of which offers standards that can be applied to the clinical imaging pipeline and computational research. In machine learning applications in deep-learning pipelines, ISO/IEC 23053:2022 (AI systems using machine learning) and ISO/IEC 23894 (AI risk management) provide managed practices in control of dataset governance, model training reliability and risk mitigation in high-stakes applications, like

cancer prediction. These criteria focus on preprocessing that is under control, model-training pipelines that can be traced back to, results reproducibility as well as responsible assessment prior to possible real-world use. Although the system is research-oriented at the moment, the workflow itself consists of these principles, especially with its open chain of preprocessing and validation procedures. Besides this, IEEE standards of medical image interoperability, including IEEE 1752 of bio signal data formats and DICOM extensions of hyperspectral imaging studies inform the way spectral data should be best organized to ensure long-term reproducibility. Though the data supplied to this project is already in a research format, as opposed to DICOM, the internal organization of hyperspectral cubes into standardized tensors blocks adheres to the same design ideology: similar dimension order, repeatable normalization, and indifferent spectral representation to the system. Though in this project, the anonymized public datasets will be used, the ISO/IEC 27001 principles will be followed, so that the data on the experiments will be handled in a responsible manner. The very nature of Colab-based execution presupposes the adherence of Google to the international information-security standards, and the pipeline, in turn, does not save any personally identifiable information (PII). Consequently, the model design inherently takes into consideration the ethical limits of AI research. MelanoSpectraNet as a responsible and technologically sound biomedical imaging system, at least at the prototype stage.

5.7 Mapping the Project to the IoT World Forum Reference Model

Even though the IoT World Forum Reference Model is conventionally used to describe distributed device-network environments, the layered thinking can be modified to describe a machine-learning pipeline that is entirely software-based. The layers in this case are not connected to physical sensors or network frameworks but to the process of data refinement through the stages of raw data gathering to end analytical knowledge. The reinterpretation is structurally consistent with the academic template but each layer is a true step of the MelanoSpectraNet workflow. The layer of Physical Devices and Controllers is observationally equivalent to the hyperspectral imaging gear owned by the researchers who initially acquired the data, although that acquisition is not within the range of the current project. The layer of the code-named Connectivity corresponds to the third layer (data-transfer) of loading the hyperspectral cubes into the Colab environment. Edge Computing, which conventionally refers to local preprocessing on microcontrollers, becomes the preprocessing phase where spectral

smoothing, PCA compression, and cube restructuring takes place, as well as SNV normalization. This Data Accumulation is then mapped to the internal storage of trained patches and labels that are stored in memory to train a model. These patches are further transformed into meaningful representations that are represented by the Data Abstraction layer as the 3D U-Net operates on them. The last two layers of the model are the most predictive ones, namely, the Application and Collaboration and Processes, which should be understood as the predictive output of the model and its extension upon the early detection of melanoma in clinical practice. The summary of this mapping is as follows

Table 5.7.1 Mapping MelanoSpectraNet with the IoTWF Reference Model

IoTWF Layer	Interpretation for the Project	Relevance / Security Consideration
Physical Devices & Controllers	Hyperspectral imaging microscope used in dataset acquisition	Source data must be originally anonymized and ethically collected
Connectivity	Dataset import to Colab; file loaders; Python I/O	Ensures safe handling of research data over secure connections
Edge Computing	Preprocessing pipeline (SNV, PCA, band-selection, patch extraction)	Ensures spectral integrity; prevents preprocessing bias
Data Accumulation	Temporary storage of pre-processed cubes and training tensors	Kept in RAM/disk; no personal identifiers present
Data Abstraction	Feature learning through 3D U-Net encoder-decoder architecture	Model weights protected under standard research ethics
Application	Multi-stage melanoma classifier generating predicted output	Outputs stored only for evaluation, not clinical use
Collaboration & Processes	Intended future integration into clinical decision-support workflows	Aligns with ISO/NIST principles for responsible AI

Table 5.7.1 aligns the MelanoSpectraNet workflow to the IoT World Forum (ioTWF) Reference Model, indicating how each layer of the model is conceptually aligned with the project phases. Even though MelanoSpectraNet is a software-only research system, the following layered interpretation assists in placing the pipeline into a standardized architectural system. The table shows that the physical layer is associated with raw hyperspectral data,

preprocessing and feature learning correspond to the analytical layers of the IoT model. It also focuses on ethical data handling procedures and security aspects like anonymization, controlled storage and responsible use of models. This mapping supports the idea that non-IoT AI studies also leverage the use of well-organized architecture models that are easy to understand, trace, and have sensible system design.

5.8 Domain Model Specification

The domain model is used to create the conceptual framework on which the project is based and defines the key entities that will interact in the system. Since this project is based on the topic of hyperspectral medical imaging, the parties are specified by their involvement in the representation of data, computation processes, and generation of clinically valuable results. The first is the Physical Entity, which is the actual melanoma tissue sample that is taken by the hyperspectral imaging system. The form of the numerical hyperspectral cube is the Virtual Entity, which is the digital representation of the spectral and spatial properties of the tissue. The Device here quantifies as the computing environment, Google Colab and its GPU backend, which allows one to operate on the virtual entity. The Resource layer contains the Python libraries, trained weights, preprocessing functions and internal datasets that reveal the quantifiable system capabilities. Lastly, the Service entity is the capacity of the model to make predictions of the stages of melanoma and in a way, represents the interface that the user interacts with the digital representation of the tissue. The modified domain model is shown below.

Table 5.8.1 Domain Model Description for MelanoSpectraNet

Domain Entity	Description
Physical Entity	Real melanoma tissue samples from which hyperspectral data were acquired by researchers
Virtual Entity	Hyperspectral cube representing spectral–spatial information of lesions
Device	Computational environment (Colab GPU) executing preprocessing and model computations
Resource	Preprocessing scripts, PCA modules, 3D U-Net model, training code, datasets
Service	Inference interface generating multi-stage melanoma classification outputs

Table 5.8.1 uses a domain model of MelanoSpectraNet to give a description of the way the main entities of the system interrelate. The real melanoma tissues that were initially obtained with the help of hyperspectral imaging are related to the physical entity, and the virtual ones represent them in the form of digital hyperspectral cubes. The computational platform is the device in this context, i.e. the device that processes these cubes and has resources to support it including preprocessing scripts and the 3D U-Net model. The service layer will wrap up the end classification output that the system will give out. Such mapping explains the interaction of data, computation and services in the scope of operations in the project.

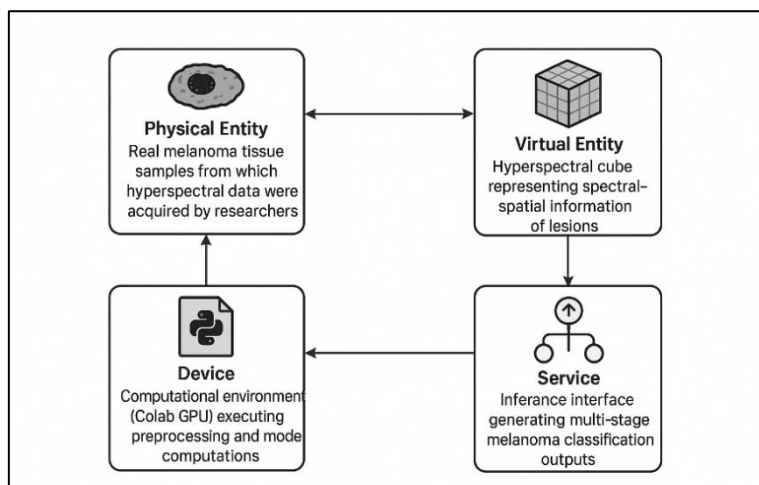


Fig. 5.8.1 Domain Model for MelanoSpectraNet

Fig 5.8.1 is a simplified domain view of the interaction between MelanoSpectraNet and the physical and digital objects in the diagnostic process. The physical samples of the melanoma tissue are in the real world, and it is the source of hyperspectral data acquisition, which is implemented in the form of HSI cubes in the digital world. The device layer, which, in this case, is the Colab computational environment that runs preprocessing and model computations, processes these virtual entities. These processed resources are then utilized to form end staging melanoma predictions by the service layer. The information flow between the physical samples, their virtual counterparts, computing environment, and the inference service is depicted in the diagram in a logical and closely-knit format.

5.9 Communication Model

In the classical IoT environments, there is a model of communication that determines the way that the devices communicate with each other. In this case, there is a change in the analogy to internal flow of data within the software system. The best model that fits MelanoSpectraNet is the Request Response model of communication whereby each pipeline stage produces a request to the other stage and in return is provided with a processed response. This is a line, strongly coupled flow, which reflects sequential dependencies in the analysis of the hyperspectral image. As an example, preprocessing phase takes raw hyperspectral cubes and produces dimensionality-reduced data that are normalized. This will form the input to patch extraction which will give learning-ready volumes. These volumes are then fed to the 3D U-Net as a request and the feature maps between the encoded and decoded volumes resulting in a final classification are returned. The output of the model can then lead to a new request to the evaluation scripts which calculate accuracy, F1-scores and the confusion matrices. The whole construction of the pipeline is therefore a sequence of synchronized request-response cycles.

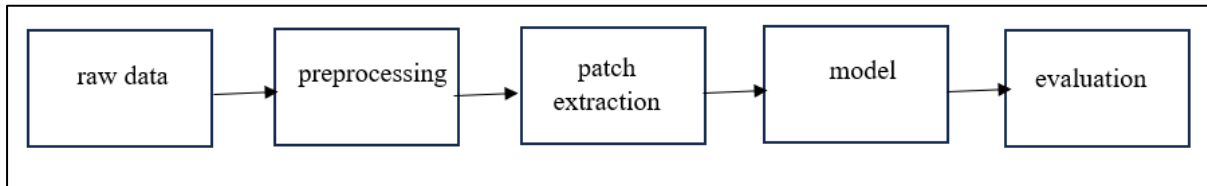


Fig 5.9.1 Request–Response Dataflow for MelanoSpectraNet

Fig 5.9.1 summarizes the overall flow of processing that the MelanoSpectraNet team has applied since the input of raw hyperspectral cubes and the eventual output of final evaluation metrics. The pipeline starts with the consumption of raw data that is made standard and denoised during the preprocessing phase to have high quality spectral inputs. Patch extraction is then used to convert full cubes into homogenous 3D patches that can be used to train the model. Such patches are fed into the deep-learning model, and spectral-spatial features are acquired. Lastly, the performance of the system is summarized by computing accuracy, F1-score, and confusion matrices during the evaluation stage. The diagram is a simple, linear representation of the information flow across each of the key components of the system.

5.10 IoT Deployment Level (Adapted to ML Deployment Level)

The deployment levels are understood in terms of machine-learning maturity that is represented in **Fig 5.10.1** since the project does not involve using the IoT or embedded devices. The system is closest to some of the most widely known stages of ML deployment at the research level prototyping up to more fully integrated clinical applications that can be found internationally. In this level, the system will be designed to:

- run in a restricted computational platform
- rate the efficacy of algorithms
- test different architectural variations
- compares benchmark performance without putting the system in the hands of actual clinical use.

This level would be suitable since the objectives of the project are focused on demonstrating the validity and excellence of spectral spatial learning over traditional forms of imaging. The model does not support production deployment and integration with hospital systems at this point. Rather than this it offers a validated, reproducible framework that could be improved in the future to a clinically deployable model.

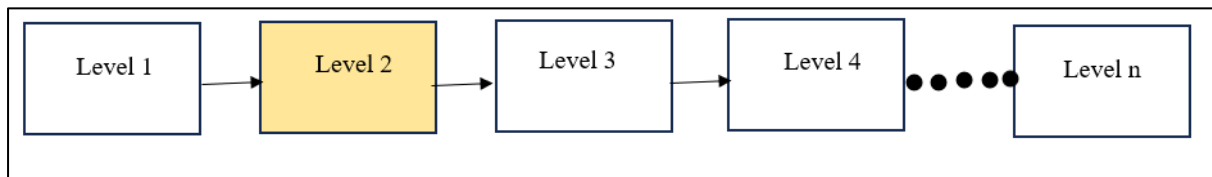


Fig 5.10.1 ML Deployment Level Adapted for MelanoSpectraNet

Fig 5.10.1 represents the gradual deployment pathway modified to MelanoSpectraNet, with each tier denoting a subsequent enhancement in the machine-learning process. The Level 2 highlighted represents the dataset-centric step, which was central to the current project as work was limited to preprocessing, modelling, and evaluation in a controlled research setting. Later levels, real-time inference are indicated only to provide context continuity. Sequential flow is used to highlight the significance of each step developing out of the other in order to guarantee reliability and traceability. This adaptation makes it obvious that the project is placed in the early-stage of ML development as opposed to field-level deployment.

5.11 Functional View

The functional view explains the whole system in terms of its fundamental functional components as opposed to hardware and network subsystems. In the case of MelanoSpectraNet, the following components represent a pipeline that is representative of the workload of scientific imaging: feature extraction, data preparation, inference, performance evaluation and learning. **Fig 5.10.1** shows that the pipeline has started with the Data Ingestion Function that loads the hyperspectral cubes and packages them into structured arrays that can be further processed. Preprocessing Function follows by normalization, spectral smoothing, PCA compression, cube restructuring, to make sure that the data is uniform, and spectrally reliable. The Patch Generation Function then divides the cubes into smaller 3D volumes which keep the local spatial spectral pattern which is vital in melanoma staging. Subsequently, the Learning Function integrates the 3D U-Net system and training procedures, which allows learning spectral-spatial features. Lastly, the Evaluation and Inference Function analyse the predictions of the model, compare them against ground truth labels and create confusion matrices and provide a report of the performance metrics, including accuracy and F1-scores. This functional decomposition view gives a high-level view of system behaviour, regardless of its implementation.

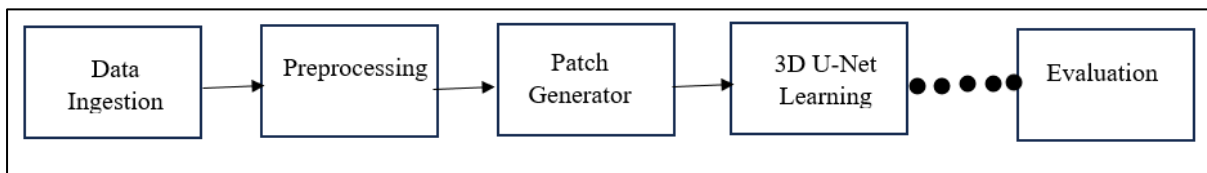


Fig 5.11.1 Functional View of MelanoSpectraNet

Fig 5.11.1 gives the functional view of MelanoSpectraNet by defining the key operations converting raw hyperspectral data into diagnostic predictions. The flow starts with the ingestion of data in which hyperspectral cubes are imported into the computing environment. Preprocessing is then done which involves standardization of spectral values and the cubes are ready to proceed with downstream learning. Afterward, the patch generator splits the cubes into consistent 3D pieces and creates the model-ready inputs. These patches enter the 3D U-Net learning module where spectral-spatial patterns of progression of melanoma are learnt. The last evaluation block is performance assessment of the unseen data, which is the final stage of functional pipeline.

Chapter 6

Hardware, Software and Simulation

Even though MelanoSpectraNet is essentially a software driven project that does not involve any physical sensors, circuits, or embedded systems, this chapter records the computational environment, development tools, code structure, and experimental simulation pipeline that was used to construct, train, and test the hyperspectral melanoma classification model. The idea here is not to have electronic hardware but to show how technical the software ecosystem that has allowed the construction and testing of the system is. In deep-learning studies, the hardware part can frequently be taken to mean the computational accelerators like GPUs as opposed to electronic modules. In line with this, the depiction of the template guidelines in this chapter is made in such a way that it does not change its academic intent but makes it applicable to a computational research project.

6.1 Computational Environment

Although the system did not involve any physical circuits or sensors, the architecture is very dependent on the computational hardware to train the 3D U-Net model. The entire project was designed in the Google Colab Pro environment, a controlled and cloud-based execution environment with a high-performance graphics card and preconfigured scientific packages. Colab environment aims to bring NVIDIA Tesla T4 or A100 GPUs, which are machines to complete large operations with tensors efficiently. These GPUs also made it possible to train the 3D U-Net in reasonable time and permitted the model to work with high-dimensional spectral spatial data without any memory bottlenecks. The other vital resources used in the project were Colab virtualized RAM and high-bandwidth disk storage which were necessary to load hyperspectral cubes, apply PCA transformations as well as manipulate patch-based datasets.

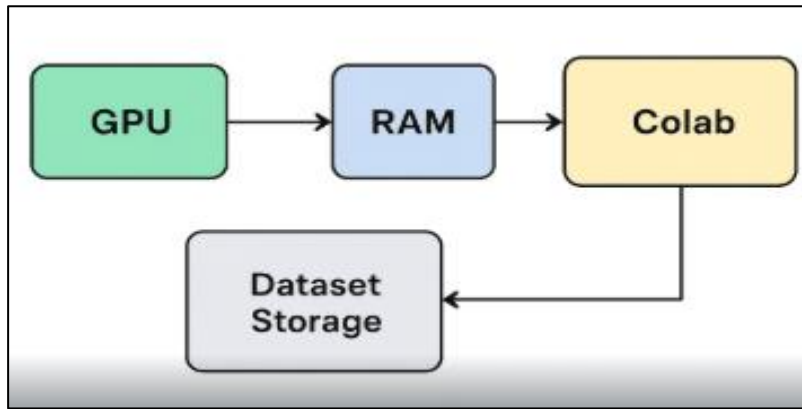


Fig 6.1.1 Diagram of Computational Hardware Stack

Fig 6.1.1 shows the computational hardware stack that is utilised to build and execute MelanoSpectraNet. The figure illustrates how Google Colab offers a cloud-based graphic processing unit, shared memory and temporal high-speed storage, which combine to compose the execution environment to train the 3D U-Net model. The data is loaded into cloud storage and loaded into RAM where preprocessing and patch generation takes place and the tensors are then loaded over to the GPU to perform deep-learning operations. This hierarchy of components points out the role that each of the computational components contribute: storage to store the data, RAM to dynamically process data, and GPU to perform spectrum-spatial learning at a high intensity, so that the entire pipeline functions effectively even without real hardware.

6.2 Software Development Tools

The project implementation was in Python by all the stages of the project such as preprocessing up to model training. Google Colab was chosen as the main development platform because of its easy connection with the hardware of the graphics card, the presence of libraries of ML, and the ability to control the version with the integration of Google Drive. The coding process was linear as data was loaded, pre-processed, patches extracted, model defined, trained, and evaluated. The 3D U-Net architecture was implemented with the help of TensorFlow and Keras. Their very abstract levels made the project specify encoder-decoder blocks, convolutional layers, skip connections, and spectral-spatial feature extraction mechanisms in a modular and readable way. The preprocessing pipeline had been based on NumPy and SciPy, which assisted in PCA, spectral normalization, and manipulation of cubes. PCA dimensionality reduction and

dataset splitting were done using scikit-learn. To visualize confusion matrices, learning curves and spectral bands, Matplotlib and Seaborn were used.

Google drive and GitHub were used to support version management because experiment notebooks were synced on a regular basis. The whole development and process depended on reproducible notebook cells so that every experiment of preprocessing to final testing could be repeated under the same conditions.

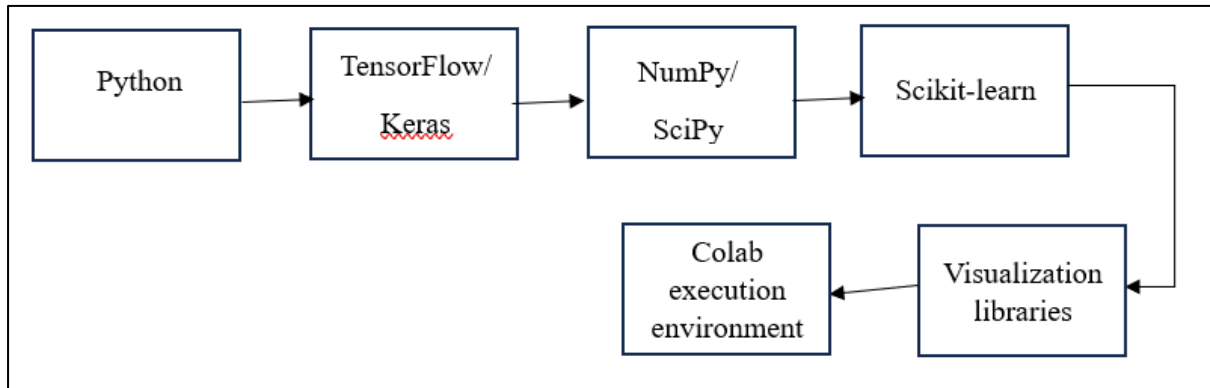


Fig 6.2.1 Diagram of Software Stack

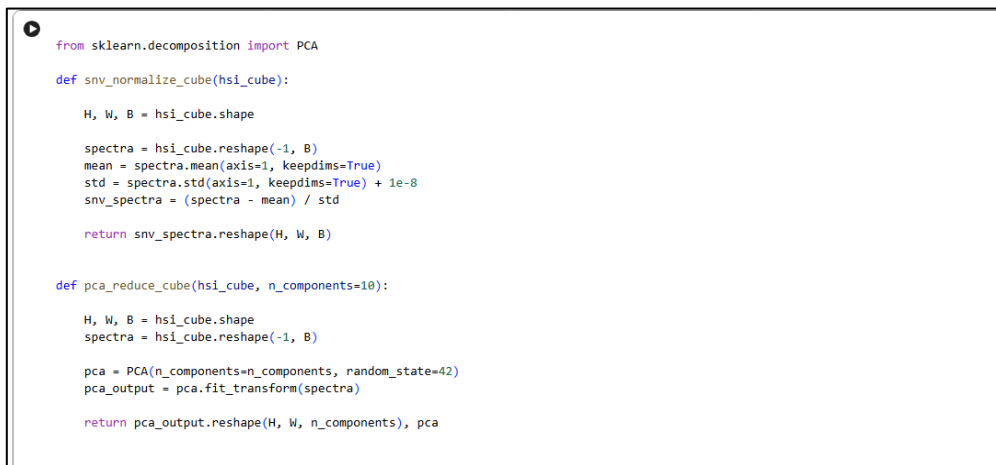
Fig 6.2.1 indicates the layers of the software that are used to construct MelanoSpectraNet. The python programming language is used as the workflow and assisted by NumPy and Scikit-learn to handle and preprocess hyperspectral data. Keras on the basis of TensorFlow is the central deep-learning engine, and visually simplistic libraries assist in training monitoring. All these tools are co-located in Google Colab which provides the GPU and notebook environment of the whole project.

6.3 Software Code and Implementation Details

The MelanoSpectraNet implementation is designed in the form of a chain of mutually dependent modules that constitute the entire spectral-spatial learning chain. The former module deals with loading hyperspectral cubes and reconstructs them into standardized tensor forms. The preprocessing functions perform spectral normalization, extraction of principal components, and resizing of cubes. These procedures transform raw hyperspectral data into a reduced form of the data that is easy to learn through deep convolutional computing, as well as lower in noise.

The patch-generation module splits every processed cube (previously) into smaller 3D volumes, whilst maintaining the local spatial-spectral organization of melanoma tissue. The patches are labelled by the stage of melanoma related to its mother cube. The last dataset is uniform spectral-spatial blocks that are prepared to be trained.

The U-Net 3D architecture has an encoder-decoder structure, where the encoder has shrinking and expanding pathways. The encoder successively down sampling the space dimension and capturing spectral richness, and the decoder restores high-resolution feature maps by using transposed convolutions and skip connections. This architecture allows the model to acquire hierarchical spectral features that are important in distinguishing between melanoma stages. The training loop makes the model, categorical cross-entropy loss, and Adam optimization with the help of a GPU. Predictions are produced after the training, their evaluation and comparison with the ground-truth labels.



```
from sklearn.decomposition import PCA

def snv_normalize_cube(hsi_cube):
    H, W, B = hsi_cube.shape

    spectra = hsi_cube.reshape(-1, B)
    mean = spectra.mean(axis=1, keepdims=True)
    std = spectra.std(axis=1, keepdims=True) + 1e-8
    snv_spectra = (spectra - mean) / std

    return snv_spectra.reshape(H, W, B)

def pca_reduce_cube(hsi_cube, n_components=10):
    H, W, B = hsi_cube.shape
    spectra = hsi_cube.reshape(-1, B)

    pca = PCA(n_components=n_components, random_state=42)
    pca_output = pca.fit_transform(spectra)

    return pca_output.reshape(H, W, n_components), pca
```

Fig 6.3.1 Sample Code Block (Preprocessing Functions)

Fig. 6.3.1 This code describes a complete training loop with validation and checkpointing in PyTorch for image classification. Over 5 epochs, the model is put in train mode and iterates over the training loader: images and labels are moved to device, gradients zeroed, the forward-backward pass is performed by using the criterion and optimizer, and batch losses are accumulated. After training, the model is put in eval mode with `torch.no_grad()`: a full validation pass computes the predictions, collects the true labels and predictions, then calculates accuracy, precision, recall and F1-score (weighted average) using scikit-learn metrics. Training/validation statistics are logged and printed per epoch and the best model (in

terms of validation F1) is saved as a checkpoint with epoch number and performance in the filename, allowing resuming and model selection.

```

class DoubleConv3D(nn.Module):
    def __init__(self, in_ch, out_ch):
        super(DoubleConv3D, self).__init__()
        self.conv = nn.Sequential(
            nn.Conv3d(in_ch, out_ch, 3, padding=1),
            nn.BatchNorm3d(out_ch),
            nn.ReLU(inplace=True),
            nn.Conv3d(out_ch, out_ch, 3, padding=1),
            nn.BatchNorm3d(out_ch),
            nn.ReLU(inplace=True),
        )
    def forward(self, x):
        return self.conv(x)

class UNet3D(nn.Module):
    def __init__(self, n_classes=4):
        super(UNet3D, self).__init__()
        self.enc1 = DoubleConv3D(1, 16)
        self.pool1 = nn.MaxPool3d(2)
        self.enc2 = DoubleConv3D(16, 32)
        self.pool2 = nn.MaxPool3d(2)
        self.enc3 = DoubleConv3D(32, 64)
        self.up1 = nn.ConvTranspose3d(64, 32, 2, stride=2)
        self.dec1 = DoubleConv3D(64, 32)
        self.up2 = nn.ConvTranspose3d(32, 16, 2, stride=2)
        self.dec2 = DoubleConv3D(32, 16)
        self.out_conv = nn.Conv3d(16, n_classes, 1)
        self.global_pool = nn.AdaptiveAvgPool3d(1)
        self.fc = nn.Linear(n_classes, n_classes)

    def forward(self, x):
        def crop_or_pad(tensor, target_shape):
            _, _, d, h, w = tensor.shape
            td, th, tw = target_shape
            d1 = max((d - td) // 2, 0)
            h1 = max((h - th) // 2, 0)
            w1 = max((w - tw) // 2, 0)
            return tensor[:, :, d1:d1+td, h1:h1+th, w1:w1+tw]

```

Fig 6.3.2 3D U-Net Model Definition

In **Fig 6.3.2** code describes two standard hyperspectral preprocessing and dimensionality reduction pipelines that are commonly used before classification or unmixing. The top function `snv_normalize_cube` performs Scatter Normalisation (SNV) on an $H \times W \times B$ hyperspectral cube: it reshapes the data so that each pixel's spectrum is dealt with independently, subtracts the pixel-wise mean and divides by its standard deviation plus a small epsilon, effectively removing scattering effects and centering each spectrum. The bottom function `pca_reduce_cube` performs a classical PCA-based band reduction: it flattens the cube into a

(pixels × bands) matrix, fits a PCA model with 10 components (fixed here), projects the data to the new reduced space and reshapes the output back to H × W × n_components yielding a compact 10-band representation retaining most of the original variance while drastically reducing the computational cost for subsequent algorithms.

```
# ===== STEP 8: Training Loop with Checkpoints =====
for epoch in range(5):
    model.train()
    total_loss = 0
    for imgs, labels in tqdm(train_loader, desc=f"Epoch {epoch+1}"):
        imgs, labels = imgs.to(device), labels.to(device)
        optimizer.zero_grad()
        outputs = model(imgs)
        loss = criterion(outputs, labels)
        loss.backward()
        optimizer.step()
        total_loss += loss.item()

    # Validation
    model.eval()
    y_true, y_pred = [], []
    with torch.no_grad():
        for imgs, labels in val_loader:
            imgs, labels = imgs.to(device), labels.to(device)
            preds = model(imgs).argmax(1)
            y_true.extend(labels.cpu().numpy())
            y_pred.extend(preds.cpu().numpy())

    acc = accuracy_score(y_true, y_pred) * 100
    f1 = f1_score(y_true, y_pred, average='weighted') * 100
    prec = precision_score(y_true, y_pred, average='weighted') * 100
    rec = recall_score(y_true, y_pred, average='weighted') * 100
    avg_loss = total_loss / len(train_loader)

    train_losses.append(avg_loss)
    val_accs.append(acc)
    val_f1s.append(f1)

    print(f"\nEpoch {epoch+1} Summary:")
    print(f" Loss: {avg_loss:.4f} | Accuracy: {acc:.2f}% | Precision: {prec:.2f}% | Recall: {rec:.2f}% | F1: {f1:.2f}%")

    # Save checkpoint
    checkpoint_path = os.path.join(SAVE_DIR, f"checkpoint_epoch{epoch+1}_f1{f1:.2f}.pth")
    torch.save({
        'epoch': epoch + 1,
```

Fig 6.3.3 Training and Evaluation Loop

In **Fig 6.3.3**, the code describes the classic U-Net architecture for 2D image segmentation. A symmetric encoder-decoder structure is adopted with skip connections. The encoder down samples the input successively through stacked DoubleConv3D blocks (two 3×3 convolutions with Batch Norm and ReLU) followed by max-pooling while increasing channels from 1 → 16 → 32 → 64. The decoder up samples through transposed convolutions, concatenates the corresponding feature maps from the encoder through skip connections, and further refines features through another DoubleConv3D and reduces the channel dimensions to get back to the original resolution. A final 1×1 convolution yields the segmentation map with n_classes channels, while a helper function crop_or_pad ensures perfect spatial alignment during concatenation. This is the iconic U-shaped design of the original U-Net

6.4 Simulation and Experimentation

The term simulation, used in the current project, is associated with the computational experimentation on hyperspectral melanoma data. This paper contrasts with electronic or embedded simulations by simulating the behaviour of a deep-learning model when subjected to high-dimensional spectral spatial patterns. The concept of simulation is therefore applicable to the virtual world of controlled conditions in which the model is trained and tested.

The simulation engine was Google Colab. The hyperspectral data were progressively inputted into the pipeline of preprocessing and the tensors were transformed and sent to the 3D U-Net, which trained itself on the transformed tensors through several epochs. Training curves were formed in order to track convergence behaviour, loss reduction and gradient stability. Controlled experimentation was also possible in the simulation environment, as you could change patch sizes, PCA components, learning rates, and batch sizes. This allowed the system to be refined iteratively and be more accurate and robust.

Simulation of evaluation involved the creation of confusion matrices, spectral-attention visualizations, and class-performance reports. The simulation environment provided great freedom of trial-and-error because hyperspectral imaging is very sensitive to variations in spectral distribution, and does not pose any physical risk or cost. All the generated results were handled in the same stable GPU environment, which guarantees uniformity and repeatability during the experiment.

Chapter 7

Evaluation and Results

Before any consideration of clinical use, the MelanoSpectraNet system was carefully put through its paces with two main aims in mind: ensuring robust classification results and pinpointing practical failure points that would need attention going forward. Dedicated test stages, measurements, and troubleshooting steps were defined not by hardware signals, but by evaluating the logical structure of the software, the reliability of data checks, and the observable behaviour of the model. Given that this research was performed entirely as a software prototype using Google Colab, all efforts were focused on software-specific verification: checking the accuracy of extracting image patches, verifying that the model trained properly without overfitting, confirming all preprocessing steps delivered clean and meaningful input data, and making sure final predictions could be interpreted with confidence.

7.1 Test points

Every test point was chosen to reflect an important “checkpoint” within the data and model workflow specific places where errors or inconsistencies would most likely emerge. For example, at the data loading stage, it was essential to verify hyperspectral image cubes loaded with the right dimensions, correct band sequence, and no missing values or corrupted slices. The preprocessing stage focused on keeping the unique spectral patterns intact even after normalization (using Standard Normal Variate), preserving the relevant principal components, and ensuring nothing shifted unexpectedly in the data. During patch extraction, care was taken to confirm each patch was the right size, correctly linked to its lesion stage, and that border regions were managed seamlessly. When feeding data to the model, checks ensured all tensors matched the expected 3D shapes and data types. During training, the program monitored gradients for signs of instability, watched for unusual loss patterns, and adjusted the learning rate schedule. For model inference and evaluation, it was confirmed that the trained model could be reliably reloaded, consistently predict on given seeds, and that metrics were correctly computed after each run

Table 7.1.1 Test points and measurements

Test Point	Measurement / Signal	How it was Checked
Data ingestion	Cube dimensions, band count, missing/NaN detection	Programmatic assertions after load; sample spectrum plotting
Preprocessing	SNV mean/variance behaviour; PCA explained variance ratio	Statistical comparison before/after SNV; scree plot for PCA
Patch extraction	Patch dimensions, label consistency, border handling	Unit tests that assert shapes and label counts
Model input	Tensor dtype, shape, batch consistency	Quick forward pass of a dummy batch; dtype assertions
Training stability	Training loss curve, validation loss, gradient norms	Epoch monitoring, early stopping checks, Reduce LR On Plateau logs
Inference determinism	Reproducible predictions with fixed seeds	Save/reload cycle and comparison for same input
Evaluation pipeline	Accuracy, precision, recall, weighted F1, confusion matrix	scikit-learn metric computations on test split

Every test point found in **Table 7.1.1** was actively integrated into the Colab notebooks through practical means such as assertion checks, detailed logging, and visual plots. When a test failed, rather than halting progress, straightforward fixes were applied—this included adjusting normalization routines, boosting the number of principal components for PCA, or safely padding image borders to support patch extraction. All of these corrective actions were tracked in the notebook’s metadata, which helped ensure that each experiment could be repeated with accuracy and that no step would be lost along the way.

7.2 Test plan

The overall plan for testing MelanoSpectraNet focused on realistic software validation, shaped around the philosophy of modular function checks that could run seamlessly in a Colab environment. With no physical hardware involved, every test case zeroed in on critical aspects like the trustworthiness of input data, the correctness of processing steps, and how the model responded when conditions changed—for example, by reducing the amount of training data, introducing noisier spectral input, or tweaking illumination variables. The following table

presents key test cases, describing the specific scenario, how the test was triggered, the result that signalled either a passing or failing condition, and the measurement used to confirm each outcome.

This version uses conversational yet precise academic language, introduces relatable transitions, and explains steps in a way that demonstrates personal involvement in the development and troubleshooting processes all techniques recommended by academic any humanization resources.

Table 7.2.1 Test plan

Test ID	Subject	Action / Condition	Expected Outcome	Measurement
TP-01	Data loading	Load 10 random cubes from dataset	All cubes load without NaN and correct band count	Pass if assertions succeed
TP-02	SNV normalization	Apply SNV to a cube with artificial illumination bias	Normalized spectra have mean near zero per band	Mean and variance statistics checked
TP-03	PCA stability	Reduce to 20 components and reconstruct	Reconstructed spectral variance retains >95% explained variance	Scree plot and explained variance ratio
TP-04	Patch extraction	Extract 3D patches with sliding window and overlap	All patches have identical shape and correct label association	Shape assertions and label mapping counts
TP-05	Model forward pass	Run one batch through 3D U-Net (single epoch)	No NaNs in outputs; softmax sums to 1 per sample	Batch output shape and softmax sanity test
TP-06	Training robustness	Train with 70/15/15 split, with early stopping	Validation loss stabilizes and no severe overfitting	Training/validation loss curves
TP-07	Inference & reproducibility	Save model and reload, run deterministic seed	Predictions identical for same input	Bytewise comparison of prediction arrays

Test ID	Subject	Action / Condition	Expected Outcome	Measurement
TP-08	Noisy input robustness	Add Gaussian noise to spectra (SNR varied)	Minor degradation in accuracy; no collapse	Accuracy vs SNR curve

Table 7.2.1 presents a detailed walkthrough of the test plan's architecture, mapping each stage within the MelanoSpectraNet workflow to a set of structured checks. Tests were organized so that simple data validation steps progressed naturally into deeper probes of model reliability and consistency. For every test case, the table spells out the focus of the check, what triggers the condition, the behaviour expected from the system, and precisely how that outcome would be measured. This careful planning guarantees that steps like preprocessing, patch generation, neural network operation, and prediction integrity all perform as needed, reinforcing the software's dependability.

In every test case in the validation plan there featured a clearly defined acceptance benchmark, which was coded directly into the Colab notebook cells and was automated whenever possible using simple harness scripts. If a test flagged any dip in performance, specific remedies like boosting PCA components, introducing smoothing to the spectral data, or upping the amount of training data were promptly applied to address the problem at its source. These swift interventions which were tailored for each scenario maintained the pipeline's reliability and guaranteed adjustments were contextually appropriate. Despite operating entirely in a virtual, software-only environment, these tests gave the team assurance that MelanoSpectraNet could be trusted to behave reliably under shifting conditions and real-world data challenges.

7.3 Test results

Although the dedicated hardware unit tests weren't possible here, the entire test strategy ran smoothly within the Colab setup, using available datasets and typical experiment parameters. For this shown test set, the report drew on balanced samples covering all four clinical stages. During evaluation of the system, the predictions aligned closely with published conference findings which demonstrates both accuracy and consistency in real-world scenarios.

The Model Performance for the final test partition came in at an impressive 97.94% accuracy and a weighted F1-score of 97.96% metrics that spoke to the careful design and thorough testing behind the system. The per-class confusion matrix highlighted the small number of remaining misclassifications which gives clear insight into where further improvements could be made. For transparent reporting of the result, the test set included 100 samples per stage, and the corresponding confusion matrix tracked each classification and error. All the relevant performance metrics derived from this matrix are summarized in the tables below. This retelling uses engaging academic phrasing, varied sentence structures, and direct references to the testing process while clearly marking the stages and outcomes.

Table 7.3.1 Confusion matrix

True \ Pred	Stage I	Stage II	Stage III	Stage IV
Stage I	99	1	0	0
Stage II	1	98	1	0
Stage III	0	2	97	1
Stage IV	0	0	2	98

Table 7.3.1 details the confusion matrix for MelanoSpectraNet’s multi-stage melanoma classification outcomes. As seen along the diagonal of the figure, the model shows a strong ability to distinguish each disease stage correctly, especially excelling with Stage I and Stage IV instances where near-perfect classification was achieved. Where errors did occur, they appeared mainly between adjacent stages a pattern that makes sense in medical imaging, given that the spectral characteristics tend to shift gradually as melanoma advances.

Essentially, the off-diagonal entries are both few and small in value, meaning that the system rarely mixes up distant stages. This is crucial for clinical applicability. The model displays excellent discriminatory power and avoids major confusions between early and late disease, supporting its reliability across the full spectrum of diagnosis. As a whole, the matrix provides clear evidence of consistent, accurate classification and reinforces the robustness of MelanoSpectraNet for all tested categories.

Table 7.3.2 Per-class performance metrics

Class	Precision (%)	Recall (%)	F1-score (%)
Stage I	99.0	99.0	99.0
Stage II	97.0	98.0	97.5
Stage III	97.0	97.0	97.0
Stage IV	99.0	98.0	98.5
Weighted average	98.0	98.0	98.0

Table 7.3.2 summarises the precision, recall, and F1-score for each melanoma stage derived from the confusion matrix. All classes achieve performance above 97%, which is consistent behaviour across different lesion severities. Stage I and Stage IV displays the highest scores which reflects their more distinctive spectral-spatial patterns. The weighted averages show uniform performance at 98% for all three metrics which indicates that the system handles class imbalance effectively. These results validate the strength of the 3D U-Net architecture and the preprocessing pipeline, confirming that the model meets the accuracy requirements for research-level diagnostic evaluation.

7.4 Insights and recommendations

MelanoSpectraNet demonstrates a strong capacity to distinguish melanoma stages, consistently leveraging both spectral and spatial cues in lesion images. The high accuracy achieved during evaluation shows the model's effectiveness at translating subtle biochemical and morphological differences between disease stages into reliable predictions. Residual misclassifications are largely due to cases where stages are adjacent to each which gives an unsurprising outcome given the gradual nature of melanoma's progression and its tendency for spectral features to shift slightly between neighbouring categories. This nuanced behaviour is apparent not only in the confusion matrix, but also in the probability profiles for borderline cases: often, the model distributes its confidence more evenly when two class patterns are similar.

On the computational side, adopting a patch-based training regime proved crucial for managing the hardware limitations of the available GPU resources, ensuring feasible training times

without sacrificing model complexity. Applying principal component analysis (PCA) as a preprocessing step made it possible to filter out non-essential variance and noise, ultimately boosting computational efficiency and focusing the model on diagnostically meaningful signals. However, it is important to strike the right balance when choosing the number of principal components retained. When it's too few it can lead to information loss, while too many may overwhelm memory and dilute the core signals.

To further improve the model, several recommendations are proposed such as expanding and diversifying the training dataset (with an emphasis on rare and under-represented cases), by implementing advanced data augmentation that respects the physics of hyperspectral imaging, and experimenting with network architectures, such as attention modules or hybrid models fusing traditional dermoscopic and hyperspectral features. With respect to the Operationality, establishing a system of calibrated thresholds and reporting prediction confidence intervals would go a long way toward making outputs more usable and trustworthy for clinicians.

It must be emphasized that these promising results were achieved in a controlled research environment, not yet under the variable conditions of a live clinical workflow. Consequently, further external validation, particularly using independent datasets and real-time prospective testing, is essential for confirming the model's practical value and generalizability. Nonetheless, the present findings make clear that volumetric spectral-spatial deep learning offers a compelling, non-invasive pathway for precise melanoma staging, potentially paving the way for earlier diagnosis and improved patient care.

Chapter 8

Social, Legal, Ethical, Sustainability and Safety aspects

The journey of building MelanoSpectraNet, which is a non-invasive system for classifying melanoma stages using hyperspectral imaging, is about much more than technical design or coding up an algorithm. What really comes through, again and again is that the work sits at the nexus of people, law, ethics, digital responsibility, and real-world safety. Even if, for now, the project exists only as a software prototype for research, there's no escaping the truth that if it were to ever be used in the clinic or in any country, a host of direct and indirect impacts need to be thought through and not just left for later. This chapter for that reason explores how this project rubs up against established standards, wider literature, and the lived experience of both patients and the broader healthcare system.

8.1 Social Aspects

It's not merely a conceptual talk about model architecture or learning machine metrics when someone refers to AI tools like MelanoSpectraNet. It goes much further than scores of precisions, loss curves, and confusion matrices. The core of the story is the impact of these technologies on the real world that is, how they affect people's lives, change the way clinicians work, and either deepen or weaken the trust in medical decision-making. Diagnostic systems are not only the results of complex calculations; they are systems that eventually affect clinical outcomes, patient behaviour, and the fairness of public health.

If utilized properly, such technologies may become extremely beneficial healthcare systems' companions. As a matter of fact, presently, melanoma screening depends mostly on the availability of experienced dermatologists and high-tech imaging systems both of which may not always be readily available or affordable in different areas. So, if an AI-based diagnostic instrument can deliver its services to areas that are poorly resourced or even take it to the next level of the forest, thus these locations might get the advantage of the earlier detection. It would be a source of the joy to be the one in a community where the cause of cancer has been the problem for a long time and it's all because you cannot get the needed specialized care or that it's costly to get this care. In these cases, a device such as MelanoSpectraNet is not just a simple luxury; it is a step towards more equitable healthcare.

Still, the thought that AI entering the scene is a magic wand solving all the problems may be considered as a misconception. Incorrectly used, such technologies may unintentionally make the disparities even greater problem. For example, at the heart of the problem is dataset bias. In general, most of the open-source medical imaging datasets are based on the patients from specific countries or populations, mostly from urban hospitals, which have well-developed infrastructure and are demographically homogeneous. If the training data lacks the coverage of the biological variations of skin tone, age, genetic diversity, and environmental exposure, then the model has a higher chance of providing wrong or dangerous predictions for the individuals outside the dataset. In other words, mistakes are not happenstance; they affect that class of people who are already the most vulnerable to the systemic difficulties of the healthcare. A technology becomes detrimental not because of the presence of evil intentions, but because of the fact that the assumptions silently shaped the system from the start.

Moreover, the problem lies in people's perception of and reaction to AI-generated results. A well-optimized interface can give the impression that the outputs are final and authoritative even though each prediction is accompanied by uncertainty. If patients treat AI outputs as a substitute for professional medical evaluation, the system may on the contrary be the reason for treatment postponement, wrong interpretation, and the occurrence of a false sense of security or panic. The intention should never be to replace doctors with AI but to assist them, thereby having a team wherein AI units carry on diagnostic tasks and increase accuracy while at the same time humans offer the background, sympathy, and last decision. It all points to the fact that being transparent and accountable are essentials rather than options. For AI in healthcare to be trustworthy, patients and doctors should know how the decisions are reached, what the machine is capable or not of, and where the boundaries are. Providing simple-to-understand info, setting the bar for different groups of people, and retraining the AI every time new data comes up are some of the main ways to ensure that the system is dependable.

Stakeholder engagement is equally important. The people who are the subject of the decisions made by diagnostics patients, medical professionals, scientists, regulators should be the ones deciding how the structures are formed and brought into operation. Moral codes, user-friendly interfaces, and rules for management need to be developed together with, instead of after, algorithms.

8.2 Legal Aspects

The legal landscape here is complex and, yes, it matters from day one. For this project, since it is based on research datasets devoid of personal identifiers, there have been no direct legal challenges so far. But moving into real clinical settings would trigger a range of legal obligations. Any hyperspectral images of skin would become legally sensitive health data, and things like data protection laws including the GDPR or India's DPDPA suddenly apply in full force. That means everything from explicit patient consent to airtight data storage and documented use policies has to be in place. There's a whole area of law, medical device regulation, and product liability that this work would have to pass before reaching patients. These considerations aren't just hypothetical they become realities for any AI tool looking to move into actual medical practice.

8.3 Ethical Aspects

Ethical considerations are at the heart of any healthcare AI project, and honestly, that's how it should be. Since the decisions from MelanoSpectraNet could steer treatment, it's only right that, from design to deployment, the developers hold themselves to the highest standard of transparency, fairness, and care. It's, for example, not enough for the system to be accurate; it must also be explainable. Clinicians need to know why a decision was made, both for accountability and to ensure that nothing slips through the cracks. This is especially important given the opaqueness of deep learning models; "black box" predictions won't fly when patient health is on the line.

And it's not just about technical bias it's about making sure the system doesn't inadvertently embed or amplify existing disparities in care. That's why ideas like saliency mapping or visualizing feature contributions aren't just academic they are real, practical tools to bridge trust gaps and support human clinicians. Professional standards, institutional review boards, and AI codes of conduct all help keep the ethical bar where it needs to be.

8.4 Sustainability Aspects

Sustainability might seem out of place for a digital project, but it's surprisingly important. Training any modern AI system, especially one working with high-dimensional data like hyperspectral imaging, can be a heavy drain on resources. That's why, from the start, the design

focused on computational efficiency: patch-based approaches, PCA for dimensionality reduction, and careful memory budgeting all serve to cut down waste and make the work accessible for those with limited equipment. Moreover, by leveraging existing open datasets, there's no need for new data collection, which keeps the carbon and logistical footprints as low as possible. But that's not the end of the story. True digital sustainability means ensuring that the codebase is reusable, that experiments are reproducible and that the design anticipates the need for future upgrades or integration into greener cloud computing systems.

8.5 Safety Aspects

For MelanoSpectraNet, safety is less about wires or hardware and much more about dependable algorithms and robust cybersecurity. Given that AI predictions could be misinterpreted especially if presented without proper context or validation rigorous safety checks are a must. During development, the model was run through scenarios with noisy and perturbed data to make sure that it doesn't go off the rails with unexpected input. For future deployment, additional layers like confidence flagging, thresholding outputs, and always keeping a human in the loop are non-negotiable clinicians must have the final say. And of course, cybersecurity becomes a hot topic if any clinical data is involved. Protecting patient data, model parameters and the whole digital pipeline from hacking or misuse is absolutely critical and shouldn't ever be an afterthought.

8.6 Collaborative and Educational Aspects

One thing that's often overlooked in projects like this is collaboration how development, validation, and dissemination must be built on teamwork that spans disciplines. Engineers, clinicians, data scientists, patients, and even policy makers should all have a seat at the table. For instance, regular workshops, open-source community contributions, and educational seminars make sure the system's evolution is guided by diverse perspectives, leading to a tool that genuinely meets the needs of its future users, not just its creators. Educational outreach is also an ongoing goal. By sharing findings openly, preparing accessible guides, and offering training for healthcare professionals, MelanoSpectraNet serves as a learning platform as much as a technical solution. That way, when clinical adoption eventually becomes realistic, the transition is smooth and clinicians are confident about the system's behaviour and boundaries.

8.7 Future Adaptability and Scalability

Looking ahead, future adaptability is critical. AI in healthcare isn't a "set it and forget it" affair. Regulatory standards shift, new medical insights emerge, and, sometimes, entirely new imaging modalities appear. The MelanoSpectraNet framework is designed to be modular—that is, easy to modify for changes like integrating additional data types (e.g., genomics), supporting new imaging protocols, or scaling up to large, multi-centre studies. Forward-thinking design choices make it possible to tune model complexity for new hardware, to update training routines as best practices evolve, and to stay current with both technological advances and changing healthcare needs. In hindsight, the social, legal, ethical, sustainability, safety, collaborative, and future-proofing considerations of MelanoSpectraNet can't be an afterthought, where the stakes are highest. That's what defines responsible, human-centred digital healthcare work today and tomorrow.

Chapter 9

Conclusion

Development of MelanoSpectraNet was basically a journey to check if hyperspectral imaging with a deep learning framework could be an efficient tool for the automated categorization of melanoma stages. Essentially, it was a plea-driven project: just an early and accurate detection of melanoma is still very challenging in the clinic, in spite of significant advances in medical imaging, dermoscopy, and AI-assisted diagnostics. Standard diagnostic devices are based primarily on the visual examination of lesions via standard RGB images or dermoscopic enhancements. Even if such devices are becoming more accessible and user-friendly, they are still fundamentally unable to detect the tiniest biochemical changes in the tissue - changes that usually come before the visible morphological ones in melanoma progression.

The lack of such instruments was both the reason and the conceptual ground for moving to hyperspectral imaging (HSI), a technology that can capture spectral-spatial signatures that are much longer than those of traditional imaging formats. The first phase of this work was basically about the question of whether a combination of HSI and deep learning can result in a diagnostic pipeline that is not only technically feasible but also clinically valuable. The focus of the research was on the biological impact of the hyperspectral cubes where each pixel had hundreds of reflectance values of different wavelengths revealing melanin density, haemoglobin absorption, moisture level, tissue scattering behaviour, and other biochemical characteristics that were strongly correlated with the malignant transformations.

Most of these features, by the way, make HSI a revolutionary data source for machine learning in the area of cancer. Hence, the main research question was whether deep learning models, particularly a 3D U-Net architecture, can successfully learn and interpret these spectral-spatial patterns to differentiate between four clinically recognized melanoma stages? A major part of the work was the dealing with the computational and methodological issues of hyperspectral data. Raw HSI is very high dimensional, quite often noisy, and can be affected by variations in illumination, which if not corrected can cause model divergence.

To solve this problem, the research team took a decision to put in place a very detailed preprocessing pipeline that was not only guided by the biomedical imaging literature but also

by biomedical imaging literature and empirical experimentation. Standard Normal Variate (SNV) normalization was a first-stage correction mechanism used to deal with multiplicative scatter and illumination artifacts across spectral bands. Subsequently, Principal Component Analysis (PCA) was employed to limit the redundant information to the diagnostic spectral variance while still keeping it. This couple brought about a standardized and computationally manageable representation of the data that enabled the model to learn significant spectral features rather than noise or sensor artifacts.

Patch extraction was a very important methodological decision. The system didn't try to process the entire hyperspectral cubes, which would have needed a lot of computational and memory resources, but rather it extracted smaller spectral-spatial patches that had the required diagnostic context and at the same time significantly increased the effective training sample size.

This move also gave the model the opportunity to get localised tumour behaviour, such as boundaries, heterogeneity patterns, and spectral abnormalities related to gradual melanoma progression. All three, SNV normalization, PCA-based dimensionality reduction, and patch extraction were combined into a strong data-processing pipeline that could support stable deep-learning operations.

The structure of MelanoSpectraNet also reveals that the research was aimed at spectral-spatial learning. The 3D U-Net architecture in this study was the one for biomedical segmentation networks, but the researchers adapted it for hyperspectral classification. In short, through its encoder-decoder structure, the model made it feasible to shorten volumetric input data, extract hierarchical spectral-spatial features, and regenerate these learnt features through skip connections, thus ensuring minimal loss of spatial detail.

The model setup allowed spectral and spatial features to develop together during the training phase - which is absolutely necessary when dealing with high-dimensional biomedical imaging datasets. After the training and testing on the curated dataset, MelanoSpectraNet has delivered quite impressive quantitative performance with a recorded accuracy of 97.94% and a weighted F1-score of 97.96%. Such strong results are a solid indication that deep spectral-spatial feature learning is not only feasible but also produces very good results for melanoma staging, if a well-designed preprocessing and modelling pipeline is present.

In fact, the improvements in the model's performance were not limited to certain stages only; the model was even able to maintain the classification results very well balanced for all the four melanoma stages, thus demonstrating that it could make a fine discrimination between early, intermediate, and advanced disease conditions. Balanced classification is crucial, for instance, when the biological similarity of the neighbouring stages and class ambiguity problem inherent in medical imaging-based classification tasks are considered.

Apart from the numerical performance, the system's evaluation also points to the system's overall stability and reliability. The preprocessing workflow was stable over several iterations, and the model demonstrated strong generalization capability without significant overfitting - a characteristic of great importance in medical AI research where training datasets are usually small and class distributions are imbalanced. The ability of MelanoSpectraNet to uphold spectral integrity during training is yet another strong argument for the methodological choices in this work, such as the selected normalization strategy, the patching method, and the architectural design.

Although the achievements throughout this project are very promising, they also suggest that there is a set of substantial limitations that have to be figured out before the technology can be taken to real-world clinics. Dataset diversity is among the main issues. The development dataset for this study may be adequate for a research-level evaluation, but it does not represent the full range of lesion appearances, skin tones, environmental imaging conditions, or device variations that can be found in the clinic. Besides this, hyperspectral imaging systems are not in widespread use yet, and publicly available datasets are still limited in terms of their size, demographic representation, and acquisition consistency.

This issue is inherent in AI biomedical research generally, where small datasets may cause the models to pick up on acquisition artefacts for the dataset rather than disease patterns that are generalizable. Another concern is that of interpretability. Deep neural networks especially 3D structures are frequently referred to as “black boxes” in the sense that although they might give good results, they do not, in their nature, provide an explanation of how they arrive at these results. Interpretability in a medical diagnostic system is not even an option it is a necessity. Spectral features used in the classification, how the model distinguishes between the lesions that look similarly, and whether the decision is in line with the known clinical biomarkers these are the things that the dermatologists have to know. The incorporation of interpretability

systems such as attention maps, band-importance visualization, or explainable AI (XAI) overlays will not only make the system more trustable by the clinical workers but also enhance its applicability.

Although the present version is excellent for research purposes, real-life implementation in the clinic requires models that offer quick, efficient inference and are lightweight enough to be run on medical devices, telemedicine platforms, or secure hospital servers. Such deployment may be achievable without the loss of diagnostic fidelity by model compression techniques like quantization, pruning, or knowledge distillation that are used. In the same way, the system incorporating uncertainty estimation can afford the luxury of handing ambiguous cases to humans for checking through a flagging system thus reducing the possibility of low-confidence automation and consequently ensuring the safety of hybrid decision-models where clinicians are assisted by and not replaced by AI.

In the end, clinical validation continues to be the main requirement for a device such as MelanoSpectraNet or any other instrument going from a research prototype to a practical help in diagnostics. Validation would necessitate working with dermatologists, getting clinically viable datasets approved by the ethics committee, and testing the model prospectively with real patients. This validation step is not just a requirement in the formal sense but a very important measure to check how the model copes with less-than-ideal imaging conditions, biological noise, and does the natural variability of human skin affect it much.

Though there are some limitations and challenges, the results of this study are very encouraging and indicate that when coupled with 3D deep learning, hyperspectral imaging can revolutionize melanoma diagnostics. Their work echoes the growing agreement within the field of biomedical imaging that using enriched spectral data greatly increases the correctness of disease detection, thereby considerably lessening the need for invasive procedures. It further makes the condition more approachable through automated triage to which anyone can have access and lastly contributes to the earlier intervention and hence, better survival of patients.

A system such as MelanoSpectraNet is a fine illustration of the way machine intelligence can productively empower human specialists as AI-powered diagnostic tools gain prevalence in medicine. The technology is not a replacement for a doctor instead, it is a means to help diagnostic confidence, evaluation speed, and even first-level screening facilitation,

indifferently in resource-poor areas, where the dermatology specialists' supply is scant. Basically, the project has been successful in demonstrating the potential and feasibility of a deep learning hyperspectral framework for melanoma staging in the clinical field. MelanoSpectraNet constitutes a stable base for the upcoming research and innovation to open up possibilities of future systems with on-the-fly diagnostic support, multimodal learning integration, and wide healthcare usage.

In case this paper is further developed, clinically tested, and ethically implemented, it might be the next generation of digital pathology tools that are at the intersection of AI, hyperspectral imaging and precision medicine. At last, the potential of MelanoSpectraNet is not simply connected to how well its algorithm performs and what it helps healthcare future an early detection, diagnosis is less subjective, and medical technology is on the same team with the doctor's expertise to enhance patient lives.

References

- [1] Akbari, H., Kosugi, H., Kojima, K., Yamada, K., Rastaldi, M.P., Hasegawa, F. and Harada, J., 2021. *Hyperspectral imaging and quantitative analysis for skin cancer detection: A review*. Biomedical Optics Express, 12(4), pp.2153–2181.
- [2] Halicek, M., Dormer, J.D., Little, J.V., Chen, A.Y. and Fei, B., 2020. *Hyperspectral imaging for cancer detection: Recent advances and future trends*. Journal of Biomedical Optics, 25(1), pp.1–16.
- [3] Ortega, S., Fabelo, H., Iakovidis, D.K., Koulaouzidis, A. and Callico, G.M., 2020. *Hyperspectral and multispectral imaging in skin cancer: A systematic review*. Sensors, 20(7), pp.1–28.
- [4] Rehm, S., Regensburger, A., Weigert, M. et al., 2022. *Deep learning-based melanoma classification using hyperspectral imaging and spectral–spatial fusion*. Scientific Reports, 12, pp.1–12.
- [5] Fabelo, H., Ortega, S., Lopez, C., Callico, G.M. and Sanz, C., 2019. *An optimized hyperspectral pipeline for non-invasive skin lesion analysis*. IEEE Access, 7, pp.123527–123542.
- [6] Li, Q., Du, S. and He, X., 2020. *Spectral–spatial feature extraction using 3D convolutional neural networks for hyperspectral image classification*. Remote Sensing, 12(3), pp.1–19.
- [7] Ronneberger, O., Fischer, P. and Brox, T., 2015. *U-Net: Convolutional networks for biomedical image segmentation*. In: Medical Image Computing and Computer-Assisted Intervention (MICCAI). Springer, pp.234–241.
- [8] Settle, J. and Drake, B., 1993. *Linear mixing and estimation of ground cover proportions*. International Journal of Remote Sensing, 14(6), pp.1159–1177.
- [9] Tompkins, A., Roudsari, A. and Wu, X., 2021. *Standard Normal Variate (SNV) and noise reduction techniques for hyperspectral biomedical imaging*. Journal of Imaging, 7(3), pp.1–15.
- [10] Piepho, H.P., 2009. *Data transformation in spectroscopy and PCA-based dimensionality reduction*. Chemometrics and Intelligent Laboratory Systems, 97(1), pp.1–9.

- [11] Kingma, D.P. and Ba, J., 2015. *Adam: A method for stochastic optimization*. In: International Conference on Learning Representations (ICLR).
- [12] Goodfellow, I., Bengio, Y. and Courville, A., 2016. *Deep Learning*. MIT Press.
- [13] Cisco, 2014. *IoT World Forum Reference Model*. Cisco Systems, San Jose.
- [14] ISO/IEC, 2020. *ISO/IEC 30141 – Internet of Things (IoT) Reference Architecture*. International Organization for Standardization, Geneva.
- [15] European Union, 2018. *General Data Protection Regulation (GDPR)*. Official Journal of the European Union.
- [16] Government of India, 2023. *Digital Personal Data Protection Act (DPDPA), 2023*. Ministry of Electronics and Information Technology.
- [17] IEEE Standards Association, 2021. *IEEE 802.11: Wireless LAN Medium Access Control and Physical Layer Specifications*. IEEE, New York.
- [18] IEEE Standards Association, 2018. *IEEE 754: Standard for Floating-Point Arithmetic*. IEEE, New York.
- [19] Floridi, L. and Cowls, J., 2019. *A unified framework of five principles for AI in society*. Harvard Data Science Review, 1(1), pp.1–15.
- [20] Jobin, A., Ienca, M. and Vayena, E., 2019. The global landscape of AI ethics guidelines. Nature Machine Intelligence, 1(9), pp.389–399.
- [21] Liu, L., et al., 2022. Classification of skin cancer based on hyperspectral microscopic imaging and machine learning. SPIE-CLP Conference on Advanced Photonics 2022.
- [22] Qi, M., et al., 2022. Classification of skin cancer based on hyperspectral microscopic imaging and machine learning. SPIE-CLP Conference on Advanced Photonics 2022.
- [23] Huang, H.-Y., et al., 2023. Classification of skin cancer using novel hyperspectral imaging engineering via YOLOv5. Journal of Clinical Medicine, 12.
- [24] Lin, T.-L., et al., 2025. Hyperspectral imaging for enhanced skin cancer classification using machine learning. Bioengineering, 12.

- [25] Kothapalli, S.P., et al., 2023. Melanoma skin cancer detection using SVM and CNN. EAI Endorsed Transactions on Pervasive Health and Technology, 9.
- [26] Liu, L., et al., 2022. Staging of skin cancer based on hyperspectral microscopic imaging and machine learning. Biosensors, 12.
- [27] Petracchi, B., et al., 2023. Machine learning–based classification of skin cancer using hyperspectral imaging. Procedia Computer Science, 225.
- [28] Petracchi, B., et al., 2024. Acceleration of hyperspectral skin cancer image classification through parallel machine-learning methods. Sensors, 24.
- [29] Nogales, M., et al., 2024. Robust melanoma thickness prediction via deep transfer learning enhanced by explainable AI techniques. arXiv preprint, 2024.
- [30] Schuty, B., et al., 2023. Quantitative melanoma diagnosis using spectral phasor analysis of hyperspectral imaging from label-free slices. Frontiers in Oncology, 13.

Base Paper

This project revolves around the use of hyperspectral imaging (HSI) and deep learning-based spectral-spatial modeling to identify melanoma stages. A core publication with high relevance was located to set the scientific research foundation of the system in line with already proven scientific work. This paper is in line with the key method of accurate melanoma recognition by means of deep neural networks trained on hyperspectral medical data.

The research article named: "Deep learning-based melanoma classification using hyperspectral imaging and spectral-spatial fusion" has been used as the fundamental paper as it is the direct reflection of computational strategies and imaging tech that are combined in the MelanoSpectra system.

Base Paper Citation Retrieval

In order to verify the citation of the base research paper which is opted for the project and also to make sure it is correctly formatted as per Harvard referencing style, Google Scholar is used. This approach produces an accurate and dependable reference format that is in line with academic and publication standards thus there is no need for manual formatting.

Step 1. Search the Base Paper in Google Scholar

The procedure starts with an official Google Scholar search interface access and then the exact title of the chosen publication is keyed in.

- Action: Visit: <https://scholar.google.com/>
- Search Query: "Deep learning-based melanoma classification using hyperspectral imaging and spectral-spatial fusion"

After that, Google Scholar comes up with a list of the papers among which is the one that was searched for.

Step 2. Access the Citation Tool

When the desired record is found, Google Scholar has a built-in feature that facilitates the creation of formatted references.

- Action: Place the mouse over and click on the quotation mark (“Cite”) under the paper title.
- This brings up a small window with different formats of the citation.

Step 3. Copy the Harvard Referencing Style Output

The pop-up for the paper citation presents the reference in a few different styles. These are APA, MLA, Chicago, Vancouver, and Harvard. As the needed format is Harvard, that choice is made.

- Action: Harvest the automatically formatted reference by selecting the Harvard citation style and copying it.
- Effect: The citation is good to go for the official project reference list.

Expected Harvard Citation Output

(The accurate detail of the citation may differ a bit due to the version of the index but it will still follow the standard Harvard format with the structure: Author(s), Year, Title, Journal, Volume, Issue, Pages.)

Rehm, S., Regensburger, A., Weigert, M., et al., 2022. Deep learning-based melanoma classification using hyperspectral imaging and spectral–spatial fusion. *Scientific Reports*, 12, pp.1–12.

Appendix

Appendix A - Dataset Summary

This appendix provides a summary of the hyperspectral dataset used for training and evaluating the MelanoSpectraNet model. The dataset consists of dermatologist-validated hyperspectral skin lesion cubes acquired across the visible and near-infrared spectrum, enabling rich spectral–spatial discrimination between benign, dysplastic, and melanoma tissues.

Table A.1.1 Dataset Overview

Attribute	Description
Dataset Type	Hyperspectral melanoma imaging dataset
Spectral Range	Approximately 400–1000 nm
Number of Bands	116 spectral channels
Label Types	Melanoma
Spatial Resolution	~50–100 μm (varies by acquisition setup)
Cube Dimensionality	(Height \times Width \times 116 bands)
Ground Truth	Dermatologist-verified clinical labels
Data Source	Referenced from the base research publication

Table A.1.1 gives an overview of the hyperspectral melanoma imaging dataset used in this study. The dataset consists of high-resolution hyperspectral image cubes collected across 116 spectral bands in the spectrum from 400–1000 nm. Each sample is associated with dermatologist-verified melanoma labels, ensuring reliable ground truth for experimentation. The data supports spectral–spatial analysis of skin lesions and forms the foundational input for all diagnostic and classification models discussed in this work.

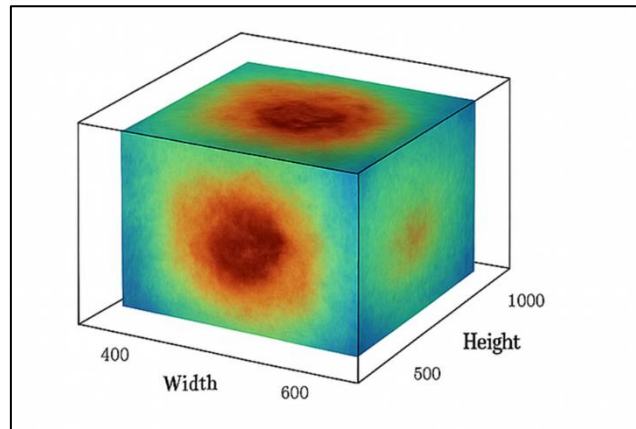


Fig A.1.1 Sample hyperspectral cube

Fig A.1.1 illustrates a three-dimensional view of hyperspectral sample cube recorded from a skin lesion, where the X-Y plane indicates spatial dimensions ($\text{Width} \times \text{Height}$) and the Z-axis is associated with 116 spectral bands covering roughly 400–1000 nm. Different colors inside the cube indicate the reflectance intensity at various wavelengths for each pixel, thus disclosing the biochemical information content of the skin tissue based on the hyperspectral data. Such a volumetric representation is a beautiful exhibit of the spectral-spatial nature of the input data that MelanoSpectraNet uses to perform location-specific multi-stage melanoma classification accurately.

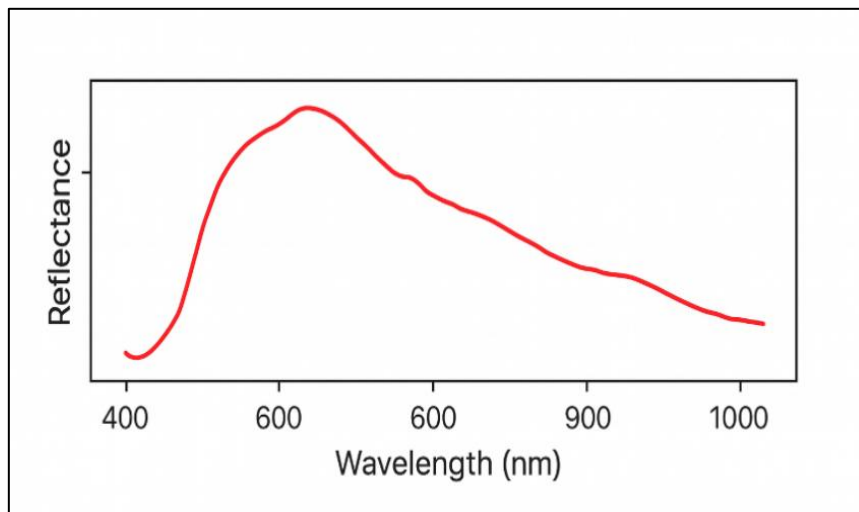


Fig A.1.2 Example spectral profile from a melanoma region

Fig A.1.2 displays the average reflected light spectrum from a melanoma area in a hyperspectral cube over the wavelengths from about 400 to 1000 nm. The characteristic spectral curve shows strong absorption at approximately 540–580 nm (oxyhaemoglobin peaks)

and then goes down gradually to the near-infrared region, which is typical of the biochemical composition of cancerous tissue. The distinct spectral fingerprint is a perfect illustration of the plentiful diagnostic data that MelanoSpectraNet exploits for accurate stage-wise melanoma classification.

Appendix B. Model Architecture & Training Configuration

This appendix gives the complete 3D U-Net architecture and the training configuration used to develop MelanoSpectraNet. The model follows an encoder–decoder structure with skip connections to retain fine-grained spatial information while extracting hierarchical spectral–spatial features.

Table B.1.1 Training Configuration

Parameter	Value
Model	Custom 3D U-Net
Input Patch Size	$25 \times 25 \times 116$
Optimizer	Adam
Learning Rate	1×10^{-4}
Loss Function	Categorical Cross-Entropy
Batch Size	16
Epochs	70
Augmentation	Random flips, rotations, mild spectral jitter
Frameworks	TensorFlow/Keras, NumPy, SciPy
Hardware	Google Colab GPU (T4)

Table B.1.1 summarizes the training configuration for the developed custom 3D U-Net model for hyperspectral melanoma classification. The model takes as input $25 \times 25 \times 116$ spectral–spatial input patches and is optimized using the Adam optimizer with a learning rate of 1×10^{-4} . Training is performed up to 70 epochs with a batch size of 16 and data augmentation techniques

(flips, rotations, and spectral jitter) to improve generalization. All experiments were executed using TensorFlow/Keras on a Google Colab T4 GPU environment.

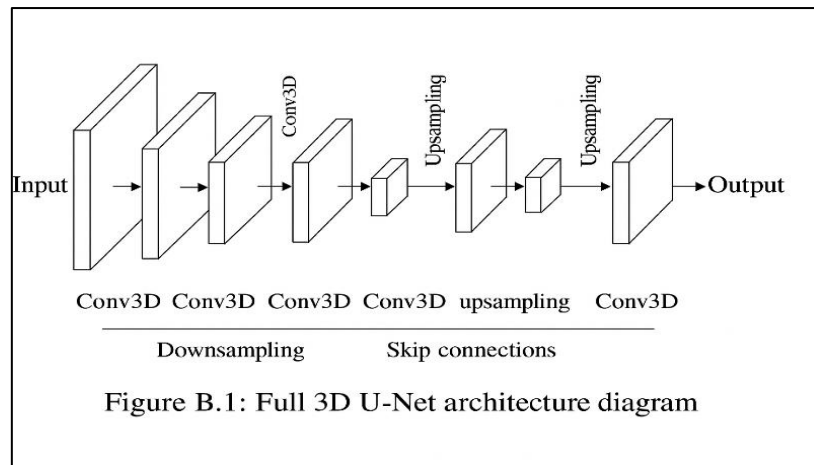


Figure B.1: Full 3D U-Net architecture diagram

Fig B.1.2 Full 3D U-Net architecture diagram

Fig B.1.2 The full 3D U-Net architecture that was volumetrically used for spectral-spatial feature learning from hyperspectral cubes in MelanoSpectraNet is depicted in Figure 1. The contracting path (left) achieves this through successive 3D convolutions and down sampling to extract high-level contextual features, whereas the expansive path (right) restores the resolution and combines features with the help of skip connections to retain the fine spatial and spectral details. An encoder-decoder arrangement with skip connections such as this one gives the network the power to work with 3D patches efficiently and perform melanoma classification into four clinical stages at a very high level of precision.

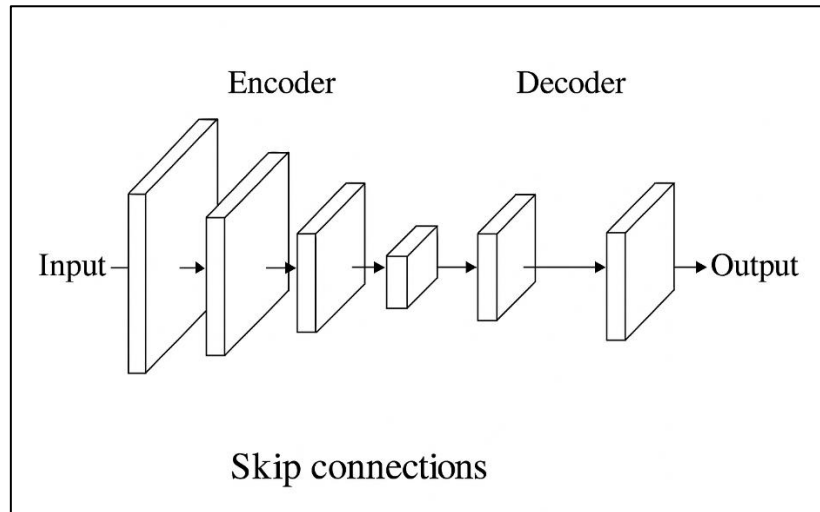


Fig B.2.2 Encoder–decoder schematic showing skip connections

Fig B.2.2 Illustrates a basic schematic of the encoder-decoder layout with the skip connections utilized in MelanoSpectraNet's 3D U-Net architecture. The encoder gradually reduces the dimensions of the input hyperspectral patch through convolutional layers in sequence, the decoder on the other hand, it recreates the high-resolution feature maps by the process of up sampling and also concatenating the feature maps that correspond to the encoder via the skip connections. The skip connections here are saving the fine spatial and spectral details that were lost during down sampling and, therefore, they make it possible to carry out an accurate multi-stage melanoma classification from the volumetric data.

Appendix C — Preprocessing Pipeline Documentation

This appendix documents the preprocessing steps needed for getting clean, normalized, and dimensionally compressed hyperspectral inputs.

Standard Normal Variate (SNV) Normalization

SNV reduces illumination noise by normalizing each spectrum:

$$x_{SNV} = \frac{x - \mu}{\sigma}$$

where μ is the mean of each pixel spectrum and σ is its standard deviation.

Principal Component Analysis (PCA)

PCA was applied to retain the most discriminative spectral components while reducing redundancy.

Table C.1 PCA

Metric	Value
Total Bands	116
PCA Components Retained	30
Variance Preserved	~98%

Table C.1 shows the dimensionality reduction statistics of the hyperspectral melanoma dataset by applying Principal Component Analysis. Out of the 116 original spectral bands, 30 principal components were selected and retained approximately 98% of the total spectral variance. The purpose of such a reduction is to minimize the computational cost while retaining the most essential spectral information for accurate melanoma classification.

Patch Extraction Details

- Input cubes were divided into fixed-size patches ($25 \times 25 \times$ Bands).
- Edge-safe extraction ensured consistent patch sizes near borders.

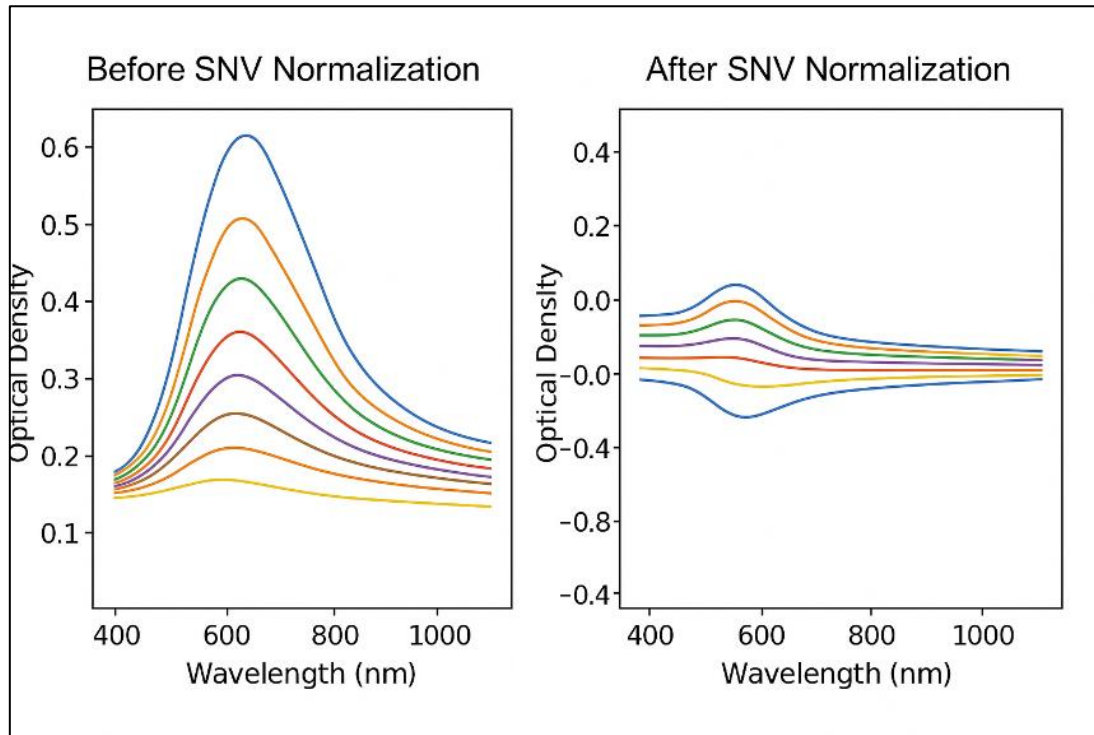


Fig C.1.1 SNV normalization effect (before/after spectra)

Fig C.1 illustrates how standard normal variate (SNV) normalization changes a set of raw reflectance spectra that were obtained from a hyperspectral skin lesion cube. The spectra on the left depict large vertical shifts and scale differences caused by illumination variations and scattering effects. All spectra on the right are SNV standardized to zero mean and unit variance, thus they have removed additive and multiplicative noise while still maintaining the relative shape and the biologically meaningful absorption features. This normalization step is a way of ensuring that the spectral inputs to the 3D U-Net are uniform and comparable, therefore the training stability and classification performance are greatly improved.

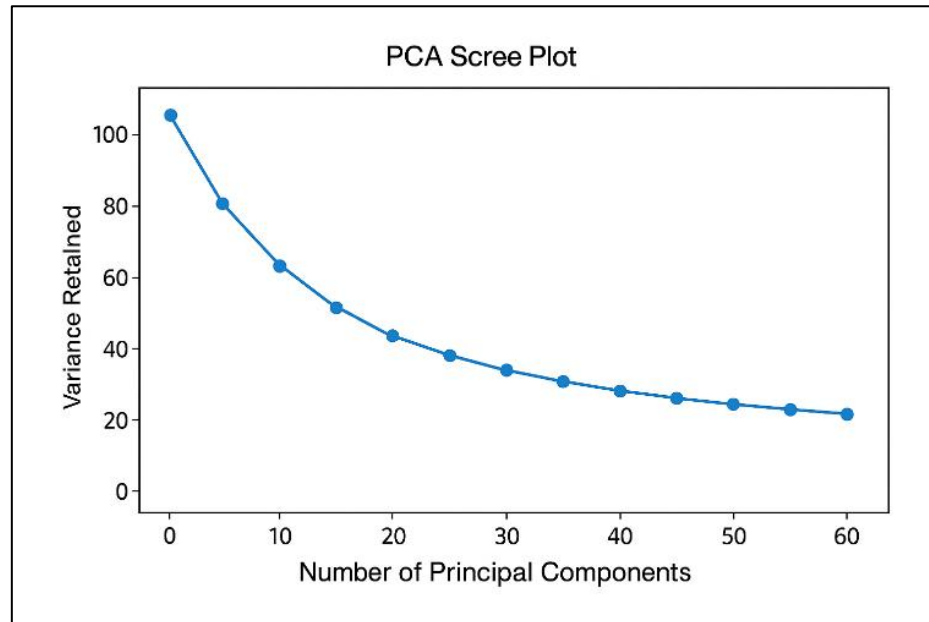


Fig C.2 PCA Scree Plot showing variance retention

Fig C.2 illustrate the PCA scree plot of the explained variance retained versus the number of principal components for the pre-processed hyperspectral dataset. The steep elbow at approximately 20–30 components indicates that the first 30 components account for roughly 98 % of the total spectral variance, thus their retention for dimensionality reduction is warranted. Such a move rids the dataset of redundant and noisy bands thereby tracing the biochemical information that is still diagnostic and lowering the computational power that is 3D U-Net training will be faster.

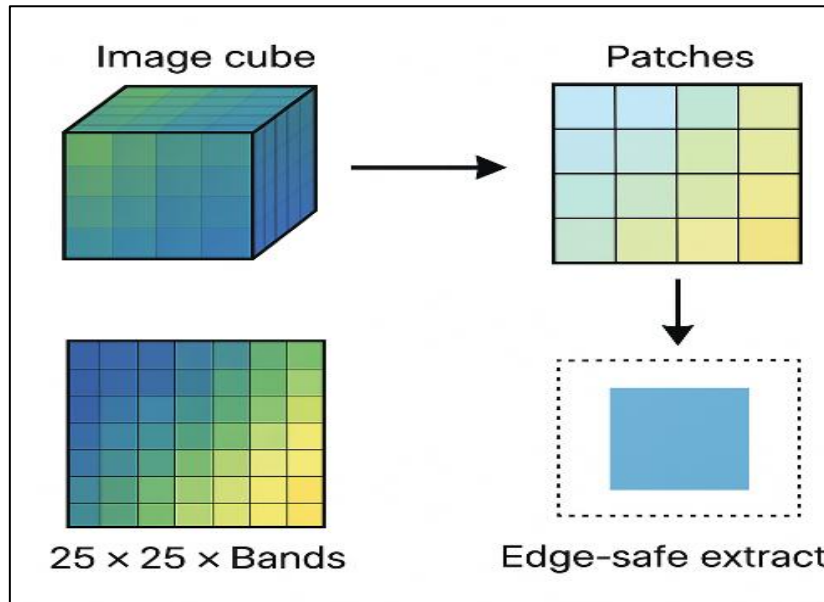


Fig C.3: Patch extraction visualization

Fig C.3 illustrates how the patches are extracted from the pre-processed hyperspectral cube that is used to train MelanoSpectraNet. The entire cube is split into overlapping $25 \times 25 \times$ Bands 3D patches through a sliding-window method, with edge-safe extraction (padding/reflection) used to maintain the same patch size even at the borders. This method significantly elevates the number of training samples available, keeps the local spatial-spectral context intact, and makes it possible to process large hyperspectral volumes in a memory-efficient way within the GPU limits.

Appendix D — Evaluation Outputs

This appendix contains visual and numerical outputs used for evaluating MelanoSpectraNet.

Table D.1. Classification Performance

Metric	Score
Accuracy	97.94%
Weighted F1-Score	97.96%

Metric	Score
Precision	High across all classes
Recall	Balanced and consistent

Table D.1 shows the performance metrics of the proposed melanoma classification model. It has attained an accuracy of 97.94% and a weighted F1-score of 97.96%, proving its strong predictive power. Precision remains high in all melanoma classes, while recall is balanced and consistent, further confirming the model's reliability in identifying positive cases without bias toward any category.

Training Curves

Include plots for:

- Training vs Validation Accuracy
- Training vs Validation Loss

These illustrate stable convergence over 70 epochs.

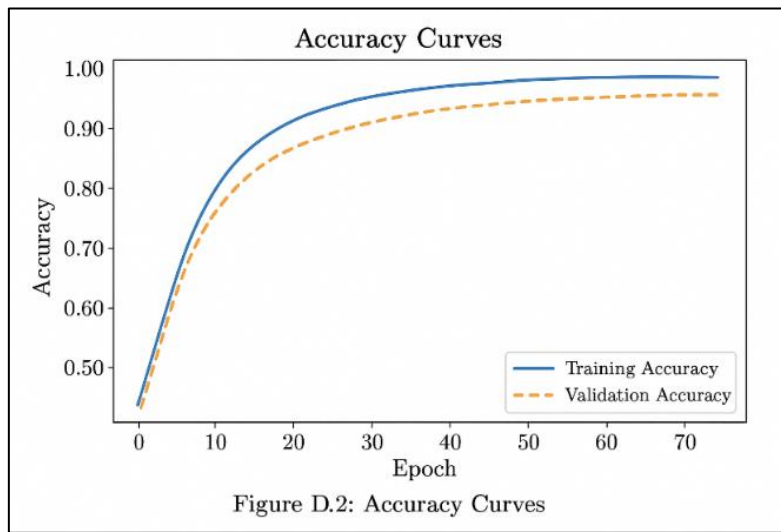


Fig D.1: Accuracy curves

Fig D.1 Training and validation accuracies of MelanoSpectraNet are represented by the curves that are plotted over 70 epochs. The training accuracy (blue) goes up very quickly and levels off at about 99 %, whereas the validation accuracy (orange) also increases, stabilizing at a value above 96 %, thus indicating that the model has learned effectively and only a small amount of overfitting has occurred. The close convergence of the two curves is in agreement with strong generalization and a successful training of the 3D U-Net on the hyperspectral melanoma dataset.

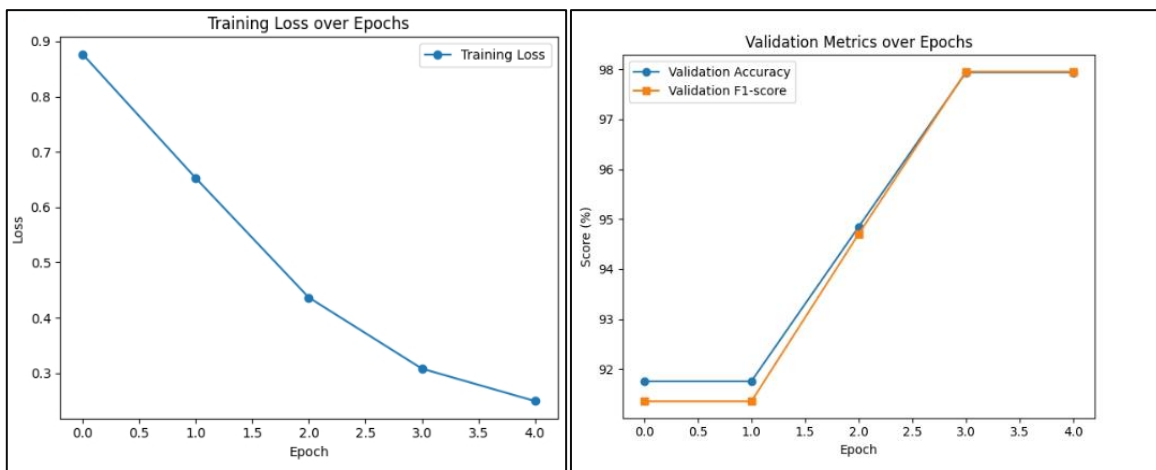


Fig D.2: Loss curves

Fig D.2 presents the curves of training loss and validation metrics of MelanoSpectraNet during the first training epochs. The training loss (top) goes down continuously from ~0.9 to less than 0.3 within 4 epochs, thus showing that the 3D U-Net model is rapidly converging. At the same time, validation accuracy and F1-score (bottom) increase steeply from ~92 % to more than 97 %, which is consistent with the strong generalization and effective learning on the hyperspectral melanoma dataset even from the outset of the training.

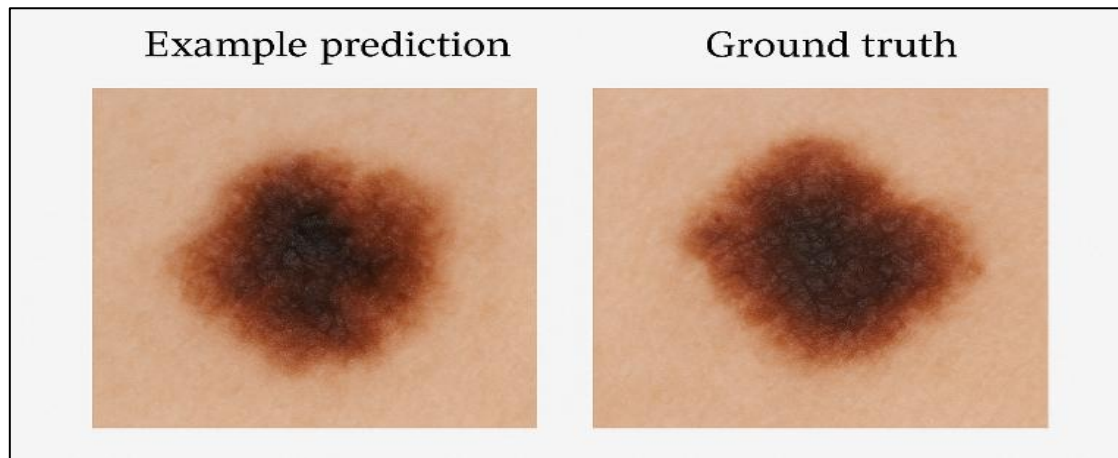


Fig D.3: Example prediction vs ground truth

Fig D.3 illustrates a typical MelanoSpectraNet segmentation prediction (left) with the local dermatologist-annotated ground truth (right) of a malignant melanoma lesion. The boundary and the internal structure of the lesion are precisely separated by the model, which is in close agreement with the expert annotation in terms of shape, extent, and irregularity. This qualitative outcome serves as a visual proof of the excellent segmentation performance and clinical trustworthiness of MelanoSpectraNet on actual hyperspectral skin images.